



Defense Threat Reduction Agency
8725 John J. Kingman Road, MS
6201 Fort Belvoir, VA 22060-6201



DTRA-TR-15-31

TECHNICAL REPORT

Assessment of Non-traditional Isotopic Ratios by Mass Spectrometry for Analysis of Nuclear Activities

Distribution Statement A. Approved for public release; distribution is unlimited.

March 2016

HDTRA1-08-1-0032

Steven Biegalski and
Bruce Buchholz

Prepared by:
The University of Texas at
Austin
1 University Station, R9000
Austin, TX 78712

DESTRUCTION NOTICE:

Destroy this report when it is no longer needed.
Do not return to sender.

PLEASE NOTIFY THE DEFENSE THREAT REDUCTION
AGENCY, ATTN: DTRIAC/ J9STT, 8725 JOHN J. KINGMAN ROAD,
MS-6201, FT BELVOIR, VA 22060-6201, IF YOUR ADDRESS
IS INCORRECT, IF YOU WISH IT DELETED FROM THE
DISTRIBUTION LIST, OR IF THE ADDRESSEE IS NO
LONGER EMPLOYED BY YOUR ORGANIZATION.

REPORT DOCUMENTATION PAGE

Form Approved
OMB No. 0704-0188

Public reporting burden for this collection of information is estimated to average 1 hour per response, including the time for reviewing instructions, searching existing data sources, gathering and maintaining the data needed, and completing and reviewing this collection of information. Send comments regarding this burden estimate or any other aspect of this collection of information, including suggestions for reducing this burden to Department of Defense, Washington Headquarters Services, Directorate for Information Operations and Reports (0704-0188), 1215 Jefferson Davis Highway, Suite 1204, Arlington, VA 22202-4302. Respondents should be aware that notwithstanding any other provision of law, no person shall be subject to any penalty for failing to comply with a collection of information if it does not display a currently valid OMB control number. PLEASE DO NOT RETURN YOUR FORM TO THE ABOVE ADDRESS.

1. REPORT DATE (DD-MM-YYYY)		2. REPORT TYPE		3. DATES COVERED (From - To)	
4. TITLE AND SUBTITLE				5a. CONTRACT NUMBER	
				5b. GRANT NUMBER	
				5c. PROGRAM ELEMENT NUMBER	
6. AUTHOR(S)				5d. PROJECT NUMBER	
				5e. TASK NUMBER	
				5f. WORK UNIT NUMBER	
7. PERFORMING ORGANIZATION NAME(S) AND ADDRESS(ES)				8. PERFORMING ORGANIZATION REPORT NUMBER	
9. SPONSORING / MONITORING AGENCY NAME(S) AND ADDRESS(ES)				10. SPONSOR/MONITOR'S ACRONYM(S)	
				11. SPONSOR/MONITOR'S REPORT NUMBER(S)	
12. DISTRIBUTION / AVAILABILITY STATEMENT					
13. SUPPLEMENTARY NOTES					
14. ABSTRACT					
15. SUBJECT TERMS					
16. SECURITY CLASSIFICATION OF:		17. LIMITATION OF ABSTRACT	18. NUMBER OF PAGES	19a. NAME OF RESPONSIBLE PERSON	
a. REPORT	b. ABSTRACT			c. THIS PAGE	19b. TELEPHONE NUMBER (include area code)

UNIT CONVERSION TABLE
U.S. customary units to and from international units of measurement*

U.S. Customary Units	Multiply by ← Divide by [†]	International Units
Length/Area/Volume		
inch (in)	2.54 $\times 10^{-2}$	meter (m)
foot (ft)	3.048 $\times 10^{-1}$	meter (m)
yard (yd)	9.144 $\times 10^{-1}$	meter (m)
mile (mi, international)	1.609 344 $\times 10^3$	meter (m)
mile (nmi, nautical, U.S.)	1.852 $\times 10^3$	meter (m)
barn (b)	1 $\times 10^{-28}$	square meter (m^2)
gallon (gal, U.S. liquid)	3.785 412 $\times 10^{-3}$	cubic meter (m^3)
cubic foot (ft^3)	2.831 685 $\times 10^{-2}$	cubic meter (m^3)
Mass/Density		
pound (lb)	4.535 924 $\times 10^{-1}$	kilogram (kg)
unified atomic mass unit (amu)	1.660 539 $\times 10^{-27}$	kilogram (kg)
pound-mass per cubic foot ($lb\ ft^{-3}$)	1.601 846 $\times 10^1$	kilogram per cubic meter ($kg\ m^{-3}$)
pound-force (lbf avoirdupois)	4.448 222	newton (N)
Energy/Work/Power		
electron volt (eV)	1.602 177 $\times 10^{-19}$	joule (J)
erg	1 $\times 10^{-7}$	joule (J)
kiloton (kt) (TNT equivalent)	4.184 $\times 10^{12}$	joule (J)
British thermal unit (Btu) (thermochemical)	1.054 350 $\times 10^3$	joule (J)
foot-pound-force (ft lbf)	1.355 818	joule (J)
calorie (cal) (thermochemical)	4.184	joule (J)
Pressure		
atmosphere (atm)	1.013 250 $\times 10^5$	pascal (Pa)
pound force per square inch (psi)	6.984 757 $\times 10^3$	pascal (Pa)
Temperature		
degree Fahrenheit ($^{\circ}$ F)	$[T(^{\circ}F) - 32]/1.8$	degree Celsius ($^{\circ}$ C)
degree Fahrenheit ($^{\circ}$ F)	$[T(^{\circ}F) + 459.67]/1.8$	kelvin (K)
Radiation		
curie (Ci) [activity of radionuclides]	3.7 $\times 10^{10}$	per second (s^{-1}) [becquerel (Bq)]
roentgen (R) [air exposure]	2.579 760 $\times 10^{-4}$	coulomb per kilogram ($C\ kg^{-1}$)
rad [absorbed dose]	1 $\times 10^{-2}$	joule per kilogram ($J\ kg^{-1}$) [gray (Gy)]
rem [equivalent and effective dose]	1 $\times 10^{-2}$	joule per kilogram ($J\ kg^{-1}$) [sievert (Sv)]

* Specific details regarding the implementation of SI units may be viewed at <http://www.bipm.org/en/si/>.

[†]Multiply the U.S. customary unit by the factor to get the international unit. Divide the international unit by the factor to get the U.S. customary unit.

**Assessment of Non-traditional Isotopic Ratios by Mass Spectrometry for
Analysis of Nuclear Activities**

August 31, 2012

LLNL-TR-577813

This work performed in part under the auspices of the U.S. Department of Energy by Lawrence Livermore National Laboratory under Contract DE-AC52-07NA27344.

DISTRIBUTION STATEMENT A. Approved for public release; distribution is unlimited.

FINAL REPORT – 2012

**Assessment of Non-traditional Isotopic Ratios by Mass Spectrometry for Analysis of
Nuclear Activities**

STEVEN BIEGALSKI, PH.D., P.E.
THE UNIVERSITY OF TEXAS AT AUSTIN
1 UNIVERSITY STATION, R9000
AUSTIN, TX 78712

BRUCE BUCHHOLZ, PH.D.
CENTER FOR ACCELERATOR MASS SPECTROMETRY
LAWRENCE LIVERMORE NATIONAL LABORATORY
MAIL STOP L-397, P.O. Box 808
7000 EAST AVENUE
LIVERMORE, CA 94551-9900

August 31, 2012

Contract #HDTRA1-08-1-0032



1.0 Objective

The objective of this work is to identify isotopic ratios suitable for analysis via mass spectrometry that distinguish between commercial nuclear reactor fuel cycles, fuel cycles for weapons grade plutonium, and products from nuclear weapons explosions. Methods will also be determined to distinguish the above from medical and industrial radionuclide sources. Mass spectrometry systems will be identified that are suitable for field measurement of such isotopes in an expedient manner.

2.0 Scope

This proposal is in support of the Basic Research Program for Combating Weapons of Mass Destruction, and the assessment of non-traditional isotopic ratios by mass spectrometry for analysis of nuclear activities. Isotopic ratios will be calculated for radionuclides produced in commercial nuclear reactor fuel cycles, fuel cycles for weapons grade plutonium, and nuclear weapons explosions. The isotopic ratios that best identify the source of the radionuclides will be selected. Isotopes with a combination of low production yields and low mass spectrometry detection limits will be removed from consideration. Mass spectrometry techniques will be evaluated as a function of their ability to detect and qualify the radionuclides of concern. A mass spectrometry system design will be identified that has the detection sensitivity necessary for the work and is capable of field operations.

Option Year 1(FY 2010) specifically focused on assessing the uncertainty and range of the results obtained in the first two years of this project. Similar calculations were performed, but utilizing more advanced codes (such as MCNPX) and different databases. Current commercial and future proposed fuel cycles were modeled. An effort will also be conducted to develop a test data set to extract forensic content from the test datasets. Both real and simulated data sets were utilized. Sample preparation methods will be developed for measurements in Option Year 2 of this project.

Option Year 2 (FY 2011) will focus on the quantification capabilities of mass spectrometry methods for the elements of choice. Forensic identification algorithms and a software tool for forensic analysis will also be developed and prototyped. Mass spectrometry measurements of the radioactive isotopes of forensic interest will be conducted.

3.0 Background

Isotopic Ratios

There are many sources for radionuclides in our environment. These include natural sources, the commercial nuclear industry, nuclear weapons, the medical industry, and other sources. Often times, the source of the radionuclide may be determined through just identification of the

radionuclide. If radionuclides are produced through different sources, the identification of the source is complex. In order to ascertain a specific source for attribution, radionuclide ratios are often employed.

Production yields of radionuclides from fission are a function of many variables including: the fissile material, the energy spectrum of the neutron flux, the magnitude of the neutron flux, and the duration of the irradiation. As a result, the ratios of certain radionuclides are highly dependent of these variables and may be utilized to distinguish between radionuclides produced from nuclear weapons, medical waste, short nuclear fuel cycles (e.g. ^{239}Pu production fuel cycles), and long nuclear fuel cycles (e.g., commercial nuclear fuel cycles). While the above is easily stated, the difficult part is to determine which radionuclide ratios should be utilized for best forensic value.

As an added complication, nuclear debris taken for forensic analysis often does not come directly from the source. There is often some type of chemical process or other process that may alter the sample composition. Chemical fractionation issues result and may significantly alter ratios of radionuclides of different elements. To mitigate this problem, it is best to examine isotopic ratios of individual elements since these ratios will be largely unaltered by chemical processes.

Mass Spectrometry

Traditional methods for radionuclide detection depend upon measuring the energy released during radioactive decay. Decay counting is relatively simple, but sample prep and analysis takes time to complete. If short-lived radionuclides have already decayed, traditional counting can be quite slow. Mass spectrometry (MS) techniques often require comparable sample prep to decay counting, but analysis is faster since MS counts atoms rather than waiting for them to decay. Reducing time between sample collection in the field and reliable analytical results requires switching to MS.

There are numerous MS techniques capable of measuring isotopic ratios. The sample size, detection limit, dynamic range, sample prep requirements, and ease of analysis vary widely among the techniques. Some techniques have very simple sample prep, requiring only dissolution in acid or combustion prior to analysis. Others require extensive preprocessing that impedes quick turnaround. In practice, the selected MS technique will need to accurately measure isotope ratios in a range of interest as quickly as possible. To insure speedy analysis, the MS technique should probably be sufficiently robust to be field deployable inside a transportainer.

Results from Current Work

Extensive work was conducted during the first two years of this project. Nuclear reactor fuel cycles were modeled utilizing ORIGEN. Fuels cycles from pressurized water reactors (PWR), boiling water reactors (BWR), and Canadian natural deuterium (CANDU) reactors were all

evaluated. Nuclear weapons were modeled by utilizing a bare sphere ($k_{\text{eff}}=1.0$) in MCNPX utilizing the BURN card. The production of every fission product, activation product, and transuranic was recorded and entered into a database.

An R value was calculated for each possible isotopic ratio. This is a metric to evaluate the forensic value. R values greater than 100 or less than 0.01 are considered good. R values are calculated as shown in equation 1.

$$R = \frac{\left(\frac{^A_Z X}{^B_Z X}\right)_{\text{Reactor}A}}{\left(\frac{^A_Z X}{^B_Z X}\right)_{\text{Reactor}B}} \quad (1)$$

Isotopic ratios were then prioritized by magnitude of the ratio, the absence of possible interferences in field monitoring, and the mass of isotope produced. Table 1 shows the isotopic ratios identified as the best for distinguishing between an unknown reactor type and a known commercial reactor signature. For this study the ratio of $^{134}\text{Cs}/^{135}\text{Cs}$ was determined to be the optimum ratio.

Table 1. Top forensic indicators to differentiate between nuclear weapons and commercial nuclear reactors.

Element	Isotope 1	Isotope 2	Present in...			A good isotopic indicator at.....				
			^{235}U sphere	Pu sphere	^{233}U sphere	1 Day	7 Days	1 Month	1 Year	10 Years
1	Cs	134	135	Y	Y	Y	Y	Y	Y	Y
2	Eu	154	156	Y	Y	Y	Y	Y	Y	N
3	Pm	147	148	Y	Y	Y	N	Y	Y	N
4	Sn	121	123	Y	Y	Y	N	N	Y	Y
5	Sm	146	151	Y	N	Y	Y	Y	Y	Y
6	Cs	134	136	Y	Y	Y	Y	Y	Y	N
7	Pm	148	149	Y	Y	Y	Y	Y	N	N
8	Ag	108	110	N	Y	N	Y	Y	Y	N
9	Ag	110	111	Y	Y	Y	Y	Y	N	N
10	Pm	148	151	Y	Y	Y	Y	Y	N	N
11	Tb	160	161	Y	Y	Y	Y	Y	N	N
12	Eu	154	157	Y	Y	Y	Y	N	N	N
13	Nb	94	97	Y	Y	Y	Y	N	N	N

R value calculations were also conducted on short and long nuclear fuel cycles in PWR, BWR, and CANDU reactors. The short cycle was defined as one that produces weapons grade Pu. The long fuel cycle was defined as one that was indicative of normal commercial nuclear reactor

operation. Similar to above, the ratios were then prioritized by the magnitude of the R value, the absence of possible interferences in field monitoring, and the mass of isotope produced. Table 2 shows the results for the best forensic indicators to determine fuel cycle length. The ratio of $^{146}\text{Sm}/^{151}\text{Sm}$ was determined to provide the best forensic value.

Table2. . Top forensic indicators to differentiate between commercial nuclear reactor fuel cycle length.

	Element	Isotope 1	Isotope 2	Present in...			A good isotopic indicator at.....			
				BWR	PWR	CANDU	0 Days	1 Month	1 Year	10 Years
1	Sm	146	151	Y	Y	Y	Y	Y	Y	Y
2	Ba	133	140	Y	Y	N	Y	Y	Y	N
3	Pm	145	147	N	N	Y	Y	Y	Y	Y
4	Cd	109	115	Y	Y	N	Y	Y	Y	N
5	Sm	145	151	Y	Y	Y	Y	Y	Y	N
6	La	137	140	Y	Y	N	Y	Y	Y	N
7	Ag	110	111	Y	Y	Y	Y	Y	N	N
8	Pm	145	151	Y	Y	Y	Y	Y	N	N
9	Pm	145	149	Y	Y	Y	Y	Y	N	N

As a result of the above work, Sm and Cs were identified as the best elements to focus on for nuclear forensics with mass spectrometry.

4.0 Tasks/Scientific Goals

Option Year 1 (FY 2011-2012)

Task 4.1: Utilize MCNPX to calculate isotopic ratios for PWR, BWR, and CANDU reactors. Compare results with those from ORIGEN obtained in the initial Phase of this work.

The Oak Ridge Isotope Generation and Determination code, or ORIGEN, is frequently used to determine nuclide production and fuel burn up in a nuclear reactor. This work sought to explore the effectiveness of using Monte-Carlo simulations to perform this same task. Specifically, the several reactor designs were run using MCNPX to calculate fuel burnup and fission products, as well as their respective radiogenic daughters.

This work compared nuclide production using ORIGEN and MCNPX calculations in three reactor types: the Westinghouse 17 x 17 pressurized water reactor, the General Electric 8 x 8 boiling water reactor, and the CANDU-37 reactor. Further, a simple sensitivity study was performed using the boiling water reactor to determine what effects small perturbations had on the isotopic ratios calculated.

For this task, nuclide production during fuel irradiation was determined using pre-existing reactor configurations for a simple boiling water reactor, a pressurized water reactor and a CANDU reactor. Nuclide production calculations were made after a fuel burnup of 1 month and 18 months. The cycle ratio, R_C , was determined for a number of nuclide pairs and is defined by equation 1 above.

Nuclide production was then determined using probabilistic Monte Carlo simulations, as opposed to the deterministic ORIGEN simulations also performed. This was achieved using the BURN card in MCNPX. MCNP input decks of the same three reactor types used in the ORIGEN calculations: the CANDU-37, the GE 8 x8 BWR, and the Westinghouse PWR, were used in this work. Cycle ratios were then calculated using the output of the MCNPX burnup calculations and then compared to the cycle ratios determined using the ORIGEN code.

A sensitivity study on what effects small changes in reactor parameters had on the isotope ratios was performed. The sensitivity measurements were conducted using MCNP on the boiling water reactor. Changes in power level, burn time, and initial boron concentrations, were investigated.

In order to minimize discrepancies between the MCNP nuclide production output and the results of the ORIGEN runs, efforts were made to ensure that the reactor parameters used for both the MCNPX and ORIGEN input files were the same. The following tables, tables 3-8, outline the inputted parameters used for the ORIGEN portion in this investigation. The fuel mass, type, enrichment, and also the moderator density were extracted from the respective MCNPX input decks. The parameters stipulated in the BURN card of the MCNPX input deck also matched the burnup and reactor power levels inputted into the ORIGEN run. Figure 1 illustrates the MCNPX fuel assembly models for the BWR, PWR, and CANDU models.

Table 3: Input parameters for ORIGEN simulation of BWR following 1-month burnup

FUEL TYPE	GE 8x8-4

U INITIAL MASS (g)	173,557
ENRICHMENT	3.23 w/o ^{235}U
BURNUP	2952.34 MWd/MTU
CYCLES	1
LIBRARIES	1
COOLING TIME	1 second
MODERATOR DENSITY	0.6 g/cm ³
POWER	17.08 MW
AVERAGE POWER	98.411 MW/MTU

Table 4: Input parameters for ORIGEN simulation of BWR following 18-month burnup

FUEL TYPE	GE 8x8-4
U INITIAL MASS (g)	173,557
ENRICHMENT	3.23 w/o ^{235}U
BURNUP	53142.20 MWd/MTU
CYCLES	1
LIBRARIES	1
COOLING TIME	1 second
MODERATOR DENSITY	0.6 g/cm ³
POWER	17.08 MW
AVERAGE POWER	98.411 MW/MTU

Table 5: Input parameters for ORIGEN simulation of PWR following 1-month burnup

FUEL TYPE	Westinghouse 17x17
U INITIAL MASS (g)	450,030
ENRICHMENT	4.5 w/o ^{235}U
BURNUP	1138.59 MWd/MTU
CYCLES	1
LIBRARIES	1
COOLING TIME	1 second
MODERATOR DENSITY	0.723 g/cm ³
POWER	17.08 MW
AVERAGE POWER	37.953 MW/MTU

Table 6: Input parameters for ORIGEN simulation of PWR following 18-month burnup

FUEL TYPE	Westinghouse 17x17
------------------	--------------------

U INITIAL MASS (g)	450,030
ENRICHMENT	4.5 w/o ^{235}U
BURNUP	20494.63 MWd/MTU
CYCLES	1
LIBRARIES	1
COOLING TIME	1 second
MODERATOR DENSITY	0.723 g/cm ³
POWER	17.08 MW
AVERAGE POWER	37.953 MW/MTU

Table 7: Input parameters for ORIGEN simulation of CANDU reactor following 1-month burnup

FUEL TYPE	CANDU-37
U INITIAL MASS (g)	19,832
ENRICHMENT	Natural
BURNUP	756.35 MWd/MTU
CYCLES	1
LIBRARIES	1
COOLING TIME	1 second
MODERATOR DENSITY	0.8121 g/cm ³
POWER	0.5 MW
AVERAGE POWER	2.88 MW/MTU

Table 8: Input parameters for ORIGEN simulation of CANDU reactor following 1-month burnup

FUEL TYPE	CANDU-37
U INITIAL MASS (g)	19,832
ENRICHMENT	Natural
BURNUP	1555.68 MWd/MTU
CYCLES	1
LIBRARIES	1
COOLING TIME	1 second
MODERATOR DENSITY	0.8121 g/cm ³
POWER	0.5 MW
AVERAGE POWER	2.88 MW/MTU

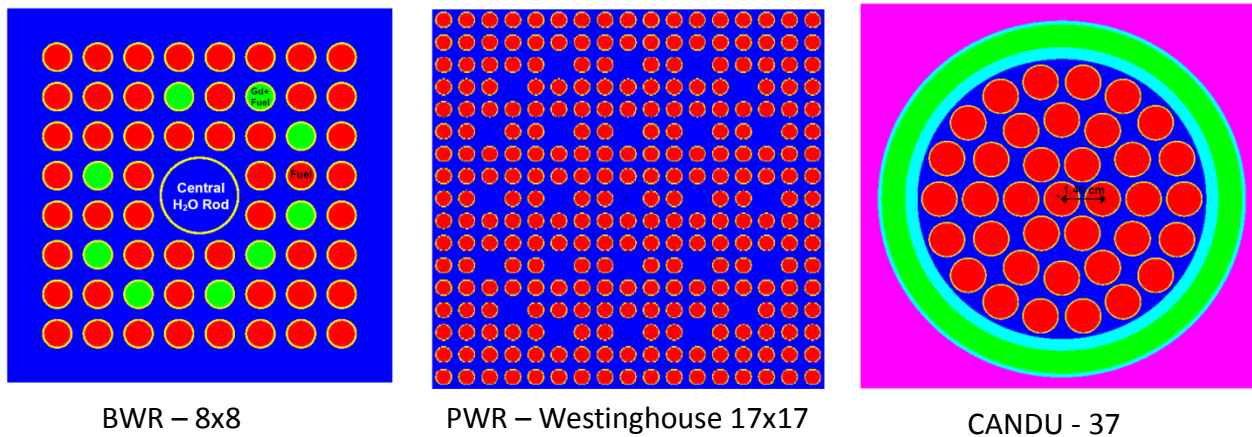


Figure 1. MCNPX models for BWR, PWR, and CANDU fuel assemblies.

The first goal of this work was to determine whether R values, as described above, have reasonable agreement for the radionuclides of interest shown in Tables 1 and 2 of this report. In addition, a sensitivity study was conducted to investigate how the R values change over a range of operational conditions. It was shown that the R values compare between the MCNPX and the ORIGEN codes. In addition, the largest operational variable that appears to affect the R values was the boron concentration in the moderator of the PWR.

Task 4.2: Develop fuel cycle models that predict forensic signatures from known generic fuel cycles

To identify isotopic ratios that could be used to differentiate short (low burnup) from long (high burnup) fuel cycles, ORIGEN-ARP within SCALE 6 was used to model several fuel types and generate expected nuclide compositions that would arise from a low and a high burnup case. Typical enrichments, specific power, and typical burnup values for commercial applications were gathered from available sources.^{1,2} From the range of typical burnup values upon discharge, representative values for a low and a high burnup case were estimated. Additionally, some simplifications to the sample parameters were made. For example, for the specific power, different values were used for the BWR and PWR classes rather than each different assembly type. All simulations were performed using “Express Mode.” The sample space is summarized in Table 9.

Table 9. Summary of Samples simulated in ORIGEN-ARP. Note, the names of the fuel types follow the convention/format of ORIGEN-ARP

Fuel Type	Reactor Type	Specific Power [MW/MTU]	Initial Enrichment [w/o]	Burnup Values [MWd/kgU]
Abb8x8-1	BWR	23	2.9	1, 27
Atrium9-9	BWR	23	2.9	1, 27
Atrium10-9	BWR	23	2.9	1, 27
CE14x14	PWR	32	2.8	1, 32
CE16x16	PWR	32	2.8	1, 32
GE7x7-0	BWR	23	2.9	1, 27
GE8x8-4	BWR	23	2.9	1, 27
GE9x9-7	BWR	23	2.9	1, 27
GE10x10-8	BWR	23	2.9	1, 27
S14x14	PWR	32	2.8	1, 32
Svea64-1	BWR	23	2.85	1, 27
Svea100-0	BWR	23	2.85	1, 27
Vver440(3.6)	PWR	32	3.60	1, 32
Vver440(3.82)	PWR	32	3.82	1, 32
Vver440(4.25)	PWR	32	4.25	1, 32
Vver440(4.38)	PWR	32	4.38	1, 32
W14x14	PWR	32	2.8	1, 32
W15x15	PWR	32	2.8	1, 32
W17x17	PWR	32	2.8	1, 32

¹ Knief, Ronald Allen, *Nuclear Engineering: Theory and Technology of Commercial Nuclear Power*, 2nd Ed., American Nuclear Society, IL: 2008

² <http://wp.ornl.gov/sci/scale/pubs/152495.pdf>

After simulation, the output files, which each contained the top 200 nuclides (by mass at discharge) were each processed to compute all isotopic ratios of the form

$\frac{^{A_Z}X}{^{A'_Z}X}$, where $A \neq A'$. Then, these ratios as defined in the statement of work were compared between the low and high burnup cases for each fuel to find R-values as shown in equation 2:

$$R = \frac{R_{low}}{R_{high}} \quad (2)$$

Lastly, R-values greater than 100 or less than 0.01, indicating two orders of magnitude change in the isotopic ratio between the two burnup values, were sought. Isotopic ratios with such R-values are identified as being good candidates for differentiating a low and high burnup fuel cycle. These identified R-values are shown in Table 10.

Task 4.3: Inverse calculations to assess forensic capabilities from test data sets

This task was comprised of three major steps: simulate fuel cycles and assemble nuclide inventories into a database, write an algorithm to compare test cases against entries in the database, assigning a figure of merit to convey their similarity and determine the best-fit entry of the database, and simulate test cases to test the identification methodology's ability to identify a known fuel cycle that best matches the unknown.

Creating the database

To run the large number of samples required for the assembly of the desired database, a MATLAB function was written that could take in parameters such as file name, fuel type, enrichment, cooling time, output units, etc. and write an ORIGEN-S input file (.inp) reflecting these parameters. Additionally, a script was written to call this function for every point in the sample space and write the required batch file to run all of the generated input files. These functions are “makeOrigenInp.m” and “makeInpsAndBat.m” (see Appendix). These files were then run with ORIGEN-S within SCALE 6. All samples were simulated at four different cooling times: 1 minute, 1 day, 30 days, and 1 year. Table 11 summarizes the sample space that was simulated. Note, the MATLAB notation for an array of values is used for denoting the burnup values: 600:690:13000 denotes the set from 600 to 13000 in steps of 690. The step sizes were chosen to correspond to roughly 1 month of operation. As in Task 4.2, these parameters were estimated from available literature to simulate some of the major differences between these different reactor/assembly types, while keeping the simulations simple.

Table 10. Summary of identified isotopic ratios useful for differentiation between low and high burnup cases. Marked are ratios having R-values larger than 100 or less than 0.01 for a particular fuel type (continued on next page).

	G E 1 0	G E 9	G E 7	Atriu m10	Atrium 9	G E 8	Ab b8	Svea 100	Svea 64	W 17	W 15	W 14	Vver 3.82	S 14	Vver 3.6	Vver 4.38	Vver 4.25	C E 16	C E 14
Pu239/Pu241	X	X	X	X	X	X	X	X	X	X	X	X	X	X	X	X	X	X	
Pu239/Pu242	X	X	X	X	X	X	X	X	X	X	X	X	X	X	X	X	X	X	
Pu239/Pu238	X	X	X	X	X	X	X	X	X	X	X	X	X	X	X	X	X	X	
Pu240/Pu242	X	X	X	X	X	X	X	X	X	X	X	X	X	X	X	X	X	X	
Nd143/Nd142	X	X	X	X	X	X	X	X	X	X	X	X	X	X	X	X	X	X	
Nd145/Nd142	X	X	X	X	X	X	X	X	X	X	X	X	X	X	X	X	X	X	
Nd146/Nd142	X	X	X	X	X	X	X	X	X	X	X	X	X	X	X	X	X	X	
Nd148/Nd142	X	X	X	X	X	X	X	X	X	X	X	X	X	X	X	X	X	X	
Nd150/Nd142	X	X	X	X	X	X	X	X	X	X	X	X	X	X	X	X	X	X	
Mo100/Mo96	X	X	X	X	X	X	X	X	X	X	X	X	X	X	X	X	X	X	
Mo98/Mo96	X	X	X	X	X	X	X	X	X	X	X	X	X	X	X	X	X	X	
Mo97/Mo96	X	X	X	X	X	X	X	X	X	X	X	X	X	X	X	X	X	X	

Mo95/Mo96	X	X	X	X	X	X	X	X	X	X	X	X	X	X	X	X	X	X
Ba134/Ba140		X	X	X	X	X	X			X	X	X	X	X	X	X	X	X
Ba136/Ba140		X	X	X	X	X	X			X	X	X	X	X	X	X	X	X
Sr89/Sr86		X	X	X	X	X	X	X	X	X	X	X	X	X	X	X	X	X
Sr89/Sr87		X	X	X	X	X	X	X	X	X	X	X		X			X	X
Te127m/Te122		X	X	X	X	X	X	X	X	X	X	X	X	X	X	X	X	X
Eu154/Eu151		X	X	X	X	X	X	X	X	X	X	X	X	X	X	X	X	X
Gd157/Gd152		X	X	X	X	X	X	X	X	X	X	X	X	X	X	X	X	X
Cd110/Cd113m		X	X	X	X	X	X	X	X	X	X	X	X	X	X	X	X	X
Nd144/Nd142			X			X		X	X	X	X	X	X	X	X	X	X	X
Xe134/Xe128								X	X				X					X
Xe131/Xe128								X	X	X	X	X	X	X	X	X	X	X
Te127m/Te124								X	X	X	X	X	X	X	X	X	X	X
Cd110/Cd115m									X	X	X	X	X	X	X	X	X	X
Am241/Am243	X														X			
Gd156/Gd157		X	X	X	X	X	X	X	X						X	X		

Xe136/Xe128							X	X										
Ba138/Ba134							X	X										
Cd111/Cd113							X	X										
Eu151/Eu152															X	X		
Gd155/Gd152															X	X		

Table 11. Summary of samples simulated in ORIGEN-ARP. Note the names of the fuel types follow the convention/format of ORIGEN-ARP.

Fuel Type	Reactor Type	Specific Power [MW/MTU]	Initial Enrichment [w/o]	Burnup Values [MWd/kgU]
Abb8x8-1	BWR	23	2.9	600:690:13000
Atrium9-9	BWR	23	2.9	600:690:13000
Atrium10-9	BWR	23	2.9	600:690:13000
CANDU28	PHWR	22	0.711	600:690:13000 ³
CANDU37	PHWR	22	0.711	600:690:13000
CE14x14	PWR	32	2.8	600:950:18000
CE16x16	PWR	32	2.8	600:950:18000
GE7x7-0	BWR	23	2.9	600:690:13000
GE8x8-4	BWR	23	2.9	600:690:13000
GE9x9-7	BWR	23	2.9	600:690:13000
GE10x10-8	BWR	23	2.9	600:690:13000
S14x14	PWR	32	2.8	600:950:18000
Svea64-1	BWR	23	2.85	600:690:13000
Svea100-0	BWR	23	2.85	600:690:13000
Vver440(3.6)	PWR	32	3.60	600:950:18000
Vver440(3.82)	PWR	32	3.82	600:950:18000
Vver440(4.25)	PWR	32	4.25	600:950:18000
Vver440(4.38)	PWR	32	4.38	600:950:18000
Vver1000	PWR	32	2.8	600:950:18000
W14x14	PWR	32	2.8	600:950:18000
W15x15	PWR	32	2.8	600:950:18000
W17x17	PWR	32	2.8	600:950:18000

To form the database, a master list of nuclides present in the 1628 samples was formed. This list includes 308 nuclides. A 308 x 1628 matrix, D, was then created, where each row corresponds to a nuclide in the master list and each column a sample. The matrix was populated as follows:

$$D_{ij} \equiv \text{Mass of Nuclide } i \text{ in Sample } j \quad (3)$$

where the nuclide index i is taken from the master list. If sample j did not have nuclide i in its top-200 list, a zero was placed in that entry of D (see “makeDTRAdatabase.m” in Appendix).

³ These burnup values are too high for CANDU reactors, but for simplicity, the same values as used for other reactors with a similar power density were used. The effects of heavy-water moderation, cross sections, etc. are still simulated.

Writing an identification algorithm

To identify an unknown fuel cycle from its top-200 nuclide list, an algorithm was written that sorts the unknown cycle’s list to agree with the master nuclide list described above (inserting zeros as appropriate), then computes a figure of merit (FOM) to describe the similarity between the resulting column vector and the 1628 columns of D. This was done by three methods:

$$FOM_1 = \sum_{n=1}^{308} (x_n - \bar{x}_n)^2 \quad (4)$$

$$FOM_2 = \sum_{n=1}^{308} |x_n - \bar{x}_n| \quad (5)$$

$$FOM_3 = \sum_{n=1}^{308} \frac{|x_n - \bar{x}_n|}{\bar{x}_n} \quad (6)$$

Here \bar{x}_n is the n th entry of the database matrix for a particular sample and x_n is the n th entry of the unknown sorted nuclide list. These three FOM’s each have a motivation: 1 is standard least-squares approach that is commonly used in many “best fit” applications, 2 adjusts the approach of 1, which may over penalize a dissimilar entry, and three adjusts this second approach to examine the relative difference in each entry in order to more fairly weight the contributions to the FOM from low concentration nuclides. In practice, an FOM is generated for each of the 1628 columns of D, and the fuel cycle (fuel type, cooling time, and burnup) with the smallest entry in the resulting vector is found to be the best fit. Additionally, an estimate of the burnup of the unknown is made by doing a linear interpolation between two samples nearest to the best-fit entry in D (which was organized to place column vectors of nuclide inventories of simulations of the same reactor and cooling time next to each other in order of burnup). The FOM was used as the notion of distance (see “IDfuelCycle.m” in Appendix).

To verify the quality of the code, samples from the database were put into the identification algorithm in order to verify that the correct column was returned as the best fit and the corresponding FOM value was 0 as would be expected. This was done using “checkDatabase.m.” In this process, it was realized that the third FOM was ill-defined (the inclusion of zeros in the database causes the FOM column vectors to have undefined entries). Rather than change the database formulation, this third FOM option was not further used.

Testing the method

To test the method, a test set of ORIGEN simulations was performed using the aforementioned MATLAB routines. These test cases featured burnup values that were not exactly represented in the database, i.e., falling in between burnup values of sample populating the database. Similar perturbations were also made on the enrichment of the fuel, cooling time of the fuel, and in the various combinations of these three variables. Table 12 summarizes. These samples were fed into the identification function for comparison against the database matrix and the results analyzed.

Table 12. Summary of the test cases used for testing the identification algorithm.

Fuel	Enrichment [w/o]	Cooling Time	Burnup [MWd/MTU]
CANDU28	0.71	1m, 7d, 30d, 1a	1400, 5000, 11000
CANDU28	0.71	3m, 9d, 2a	6120, 5000
CE 16x16	2.8	1m, 7d, 30d, 1a	1700, 8700, 17000
CE 16x16	2.8	3m, 9d, 2a	8700, 9150
CE 16x16	3.1	7d, 9d	8700, 9150
GE 7x7-0	2.9	1m, 7d, 30d, 1a	2000, 7200, 10800
GE 7x7-0	2.9	3m, 9d, 2a	7200, 8880
GE 7x7-0	3.2	7d, 9d	7200, 8880

The function “runTestCases.m” performed these tests and recorded the results. The names of the samples were parsed to find the parameters used in the simulation, and these parameters (burnup, enrichment, cooling time) were examined to determine which were perturbed versus calibrated values. The function then passed one of the test cases into the identification algorithm. Relative errors in the estimation of burnup, both from the best-fit entry of the database matrix and from the linear interpolation method, were calculated for each test case. Lastly, successes in the estimation of the fuel assembly type and cooling time were recorded. Successes in the estimation of the assembly type were defined as getting the type exactly correct, i.e., guessing that a test sample was a CE 16x16 rather than CE 14x14 was not considered a success. For a cooling time estimation to be declared successful, it had to be the closest possible guess (of which the algorithm can only make 4: 1 minute, 1 day, 30 days, and 1 year) to the actual cooling time of the unknown.

Figure 1 shows the values of FOM_1 and FOM_2 for different entries in the database, generated for one of the test cases. In this example, the simulated fuel assembly was a CE 16x16 type, with an initial enrichment of 2.8 w/o, a burnup value of 1700 MWd/MTU, and a cooling time of one year. The algorithm is able to correctly identify the type of reactor (see Figure 2.a) and then the nearest burnup value represented in the database (see Figure 2.b). Both of these identifications are indicated by a minimum in the FOM values. Note, while these FOMs are discrete functions, they are displayed with a line for ease of reading the figures. The interpolated burnup value

produced by the second FOM produces a better estimate of the burnup of the test case versus the best-fit entry from the database, with relative errors of 3.24% and 8.82%, respectively.

These and the rest of the results for test cases that only altered the burnup are given in Table 12. The complete results, as described above, became very difficult to examine, and further work is needed to fully understand underlying trends, sensitivities of the method to the different sources of variance introduced in this study, and to alter the method to better deal with these additional sources of variance. The complete results may be found in Tables A.1 and A.2 within the Appendix.

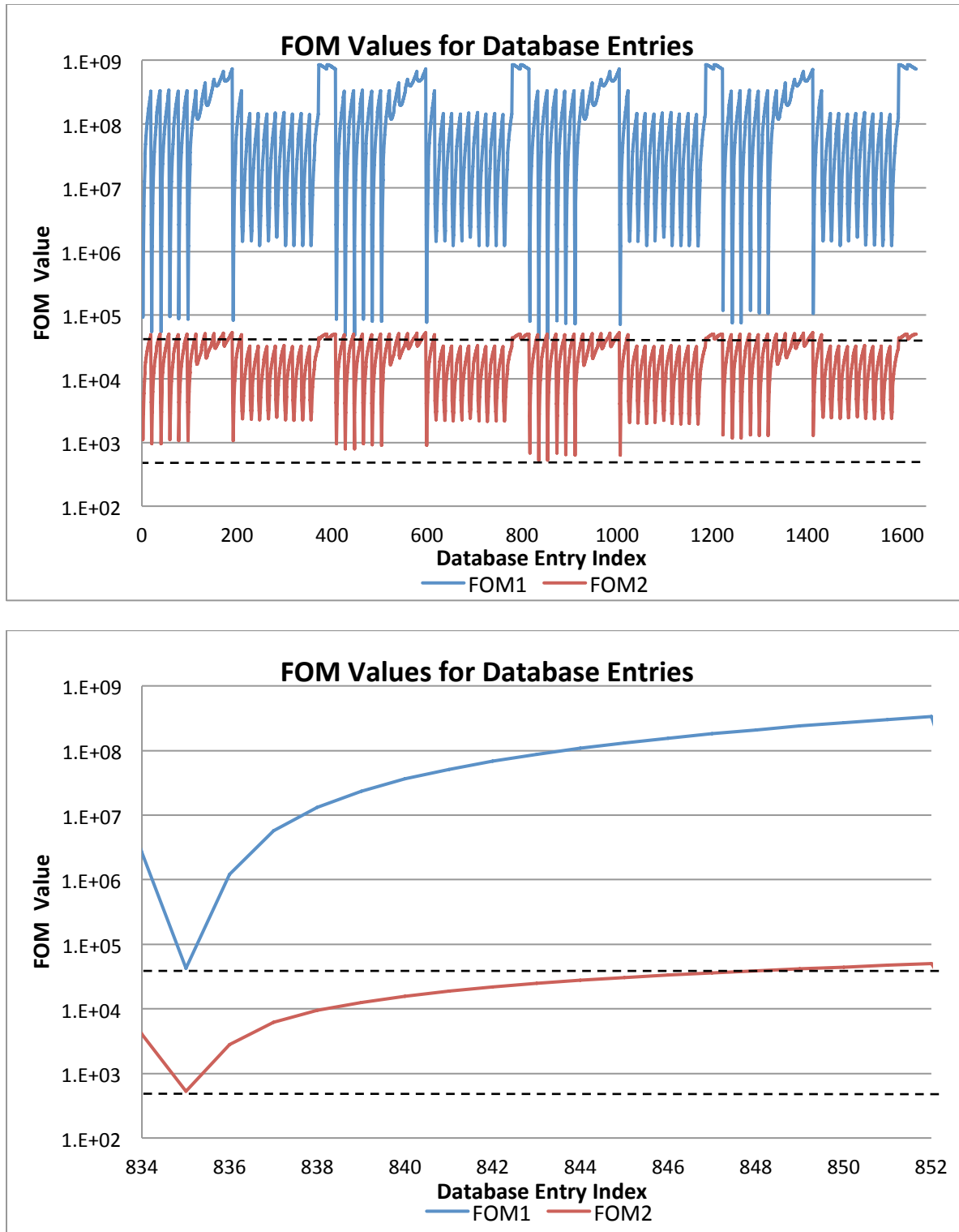


Figure 2. Values of FOM for entries in the database. **1.a:** (Top) The area around the minimum (black line) identifies the reactor type and cooling time. **1.b:** (Bottom) Shows the FOM values

for entries in the database corresponding to CE 16x16 with 1 year cooling time and minimum value for the two FOM's, identifying the best guess for the burnup of the test case.

Table 7. Shows the results of test cases where only burnup was altered. The results shown here were obtained with the least squares value figure of merit. The case corresponding to Figure 1 is highlighted and shows the same test case results as obtained using the absolute value figure of merit.

Reactor Type Guess	Simulated Reactor	Success	Best-Fit Burnup [MWd/MTU]	Error [%]	Interpolated Burnup [MWd/MTU]	Error [%]	Simulated Burnup [MWd/MTU]	Cooling Time Guess	Simulated Cooling Time	Success
CANDU28	CANDU 28	X	1290	7.86	1552	10.86	1400	1a	1a	X
CANDU 37	CANDU 28		1290	7.86	1522	8.71	1400	7d	1m	
CANDU 28	CANDU 28	X	1290	7.86	1547	10.50	1400	30d	7d	
CANDU 28	CANDU 28	X	1290	7.86	1552	10.86	1400	30d	30d	X
CANDU 37	CANDU 28		4740	5.20	5318	6.36	5000	1a	1a	X
CANDU 37	CANDU 28		4740	5.20	5301	6.02	5000	7d	1m	
CANDU 37	CANDU 28		4740	5.20	5313	6.26	5000	30d	7d	
CANDU37	CANDU 28		4740	5.20	5318	6.36	5000	30d	30d	X
CANDU 28	CANDU 28	X	10950	0.45	11046	0.42	11000	1a	1a	X
CANDU 28	CANDU 28	X	10950	0.45	11047	0.43	11000	1m	1m	X
CANDU28	CANDU 28	X	10950	0.45	11047	0.43	11000	7d	7d	X
CANDU 28	CANDU 28	X	10950	0.45	11047	0.43	11000	30d	30d	X

CE 16x16	CE 16x16	X	1550	8.82	1909	12.29	1700	1a	1a	X
CE 16x16	CE 16x16	X	1550	8.82	1889	11.12	1700	7d	1m	
CE 16x16	CE 16x16	X	1550	8.82	1905	12.06	1700	30d	7d	
CE 16x16	CE 16x16	X	1550	8.82	1909	12.29	1700	30d	30d	X
VVER 1000	CE 16x16		9150	5.17	8307	4.52	8700	1a	1a	X
VVER 1000	CE 16x16		9150	5.17	8317	4.40	8700	1m	1m	X
VVER 1000	CE 16x16		9150	5.17	8334	4.21	8700	1m	7d	
VVER 1000	CE 16x16		9150	5.17	8309	4.49	8700	30d	30d	X
W 14x14	CE 16x16		16750	1.47	17198	1.16	17000	1a	1a	X
W 14x14	CE 16x16		16750	1.47	17206	1.21	17000	1m	1m	X
W 14x14	CE 16x16		16750	1.47	17196	1.15	17000	30d	7d	
W 14x14	CE 16x16		16750	1.47	17201	1.18	17000	30d	30d	X
GE 7x7-0	GE 7x7-0	X	1980	1.00	2062	3.10	2000	1a	1a	X
GE 7x7-0	GE 7x7-0	X	1980	1.00	2054	2.70	2000	1m	1m	X
GE 7x7-0	GE 7x7-0	X	1980	1.00	2060	3.00	2000	7d	7d	X
GE 7x7-0	GE 7x7-0	X	1980	1.00	2061	3.05	2000	30d	30d	X
GE 8x8-4	GE 7x7-0		7500	4.17	6922	3.86	7200	1a	1a	X
GE 8x8-4	GE 7x7-0		7500	4.17	6913	3.99	7200	1m	1m	X
GE 8x8-4	GE 7x7-0		7500	4.17	6932	3.72	7200	1m	7d	
GE 8x8-4	GE 7x7-0		7500	4.17	6938	3.64	7200	1m	30d	
GE 7x7-0	GE 7x7-0	X	10950	1.39	10666	1.24	10800	1a	1a	X
GE 7x7-0	GE 7x7-0	X	10950	1.39	10658	1.31	10800	1m	1m	X
GE 7x7-0	GE 7x7-0	X	10950	1.39	10662	1.28	10800	7d	7d	X
GE 7x7-0	GE 7x7-0	X	10950	1.39	10669	1.21	10800	7d	30d	

The second figure of merit (absolute value) was more successful in identifying the reactor type, with 27 successes versus 19 successful identifications made by the first FOM, while the first FOM performed slightly better at predicting cooling time, the first and second FOM's yielding 25 and 24 successful cooling time guesses respectively. The average relative errors in predicting the burnup of the test cases using the best-fit entry from the database was similar for the two FOM's, the least squares averaging 3.95% and the absolute value averaging 3.99% relative error. The error in this burnup prediction is a function of the difference between the burnup values simulated for the formation of the database. Unsurprisingly, the absolute value FOM performed much better predicting the burnup of the test cases via linear interpolation, yielding an average relative error in prediction of 1.38% versus the 4.72% average produced using the first figure of merit. Thus, overall the second figure of merit performed better.

As the full set of test cases and results becomes much more complex to analyze, further work is suggested to more fully understand the performance of the method outlined in this work and develop ways to overcome its shortcomings. Possible solutions could include using different figures of merit and/or combinations of different FOM's for the various parts of the analysis. Optimization of the database, e.g., including more simulations or concentrating database entries at points in the sample space (reactor type, burnup values, enrichment, etc.) where the output is most sensitive to changes in these input parameters, could also improve the ability of the method to make accurate predictions. Similarly, the sensitivity of each nuclide in the output files relative to these input parameters could be studied and this knowledge used to optimize the method. Lastly, such a sensitivity study could also be used to make estimates of the uncertainty in the various predictions made.

In summation, the present work demonstrates the efficacy of a simple method of analyzing more of the data available from measurements of spent nuclear fuel for the purposes of fuel cycle identification. Further work is warranted to develop such methods as a complement to currently-employed methods that rely on data reduction via the use of isotopic ratios.

Task 4.4: Develop chemistry for analysis of samarium.

The chemical form of samarium required for analysis varies for different mass spectrometry techniques. Inductively Coupled Plasma Mass Spectrometry (ICPMS) requires a liquid sample for introduction into the plasma. Accelerator mass spectrometry requires solid targets for negative ion production. We previously examined ion production from samarium oxide (Sm_2O_3) and samarium fluoride (SmF_3) in the LLNL ion source. The fluoride produced an order of magnitude more negative ions and was selected as the best option for samarium AMS sample material. Samarium is readily soluble in nitric acid or hydrochloric acid and commercial elemental liquid standards contain nitric acid. Liquid Sm standards are generally produced by dissolving high purity solid Sm_2O_3 in high purity nitric acid.

Production of SmF_3 for AMS samples was investigated starting with a Sm liquid standard. This material does not have elemental interferences and is a good starting material for developing sample chemistry. The LLNL AMS facility uses the fluorides of Ca and Sr currently, so we have lab facilities suitable for working with hydrofluoric acid. The general procedure for making SmF_3 is as follows: Start with Sm solution, e.g. 4 mL solution containing 2 mg Sm in 5-10% nitric acid. Add concentrated ammonium hydroxide but keep solution acidic. Add 3 mL 40% hydrofluoric acid and allow samarium fluoride to precipitate overnight. Centrifuge to form a pellet and remove the supernatant. Add 1 mL of dilute hydrofluoric acid, then transfer samarium fluoride and rinse to a new 2 mL centrifuge tube. Centrifuge again to form a pellet, remove the supernatant, and dry overnight on a heating block. Place dry SmF_3 in a watertight vial until ready to use.

Samarium fluoride can be precipitated by adding a soluble fluoride salt such as ammonium fluoride rather than hydrofluoric acid. Ammonium fluoride has traces of hydrofluoric acid, however, so the same safety procedures are used. Hydrofluoric acid has been shown to work better when solutions are less pure (e.g., Ca), however, so we decided to stick with it.

Task 4.5: Conduct presentations/meetings at times and places specified in the contract schedule.

A presentation was delivered on July 22, 2011 in Springfield, VA at the DTRA program review.

Task: 4.6: Write Option Year 1 report

It was written and submitted by the September 1, 2011 deadline.

Option Year 2 (FY 2011)

Task 4.7 Validate mass spectrometry detection limits for identified elements.

Measurements were conducted at LLNL utilizing both AMS and ICPMS to evaluate the detection capabilities for samarium isotopes. The Sm_2O_3 sample used for irradiation appears to be extraordinarily pure samarium for a commercial material as analyzed by ICPMS. No europium or ^{151}Sm was identified in it. Scans on a pulse counting detector over mass 151 with simultaneous collection of the ^{150}Sm , ^{152}Sm and ^{154}Sm ion beams in Faraday cups showed only a relatively smooth scattered-ion tail coming from ^{152}Sm . No indication of a peak could be discerned above this baseline, which was about 50 cps at mass 151 for a 4.534×10^7 cps ion beam from ^{152}Sm . This gives an abundance sensitivity at mass 151 with respect to 152 of

approximately 1.1 ppm. The ^{150}Sm ion beam was running at about 1.257×10^7 cps, and the semi-quantitative value for $^{150}\text{Sm}/^{152}\text{Sm}$ equals 0.277, which is approximately that of normal Sm. The best estimate of a count rate that would be discernable above this baseline, the critical level, is 25 cps, and this gives a result for $^{151}\text{Sm}/^{150}\text{Sm} < 2 \times 10^{-6}$. Hence, the detection limit for ICPMS of $^{151}\text{Sm}/^{150}\text{Sm}$ is 2×10^{-6} .

AMS measurements on Sm show that limitations are dominated by an isobar of ^{151}Eu and a scattered tail of stable ^{150}Sm isotope that cannot be distinguished with the high count rates encountered. The ^{151}Eu interference may be addressed through improved chemistry. The concentration of Eu would need to be reduced from $\sim 1 \times 10^{-6}$ to 1×10^{-10} or preferably, 1×10^{-12} . The Sm stable isotope interference will be a function of stable Sm in the sample. For pure nuclear fuel samples, the stable Sm isotope interference may be manageable. For environmental samples, the magnitude of the interference largely depends on the sample makeup. Sm is a lanthanide with an average crustal composition of 8 ppm. As a result, natural Sm interference with anthropogenic Sm isotopes could cause issues depending on sample acquisition.

More discussion may be found under the discussion of Task 4.9.

Task: 4.8 Develop algorithms for forensic determinations utilizing mass spectrometry.

While isotopic ratios have been used effectively until present, a great deal of information available to the forensic analyst goes unused by these univariate approaches. Multivariate analysis has the ability to overcome difficulties that traditionally plague univariate approaches, such as poor calibration data [6]. For instance, multivariate data analysis allows for the determination of multiple analytes with a single multivariate measurement and the detection of unexpected components [7]. Multi-way analysis can additionally allow for adequate analysis of analytes in the presence of unexpected components and signals. These approaches have been widely applied in chemometrics and there is a wealth of literature on the subject [8, 9]. Additionally, the new emphasis on speed of analysis requires as much useful information to be gathered from every measurement. For these reasons, we believe that investigation into the application of multivariate data analysis techniques to nuclear forensic applications is warranted.

This work is an initial study to validate our claim that multivariate analysis could be successfully applied to nuclear forensic applications. We do this by applying nearest neighbor and ridge regression algorithms to predict the burnup and reactor type of spent nuclear fuel using simulated data.

Predictions of reactor type and burnup were made by comparing the radionuclide composition, herein referred to as the nuclide vector, of an unknown test case to a collection of vectors corresponding to known reactor type and burnup value, referred to as the training data. All the data was simulated, and the preparation of this data is described in Section 3.1.

The training data was loaded into a matrix $X \in \mathbb{R}^{N \times p}$, where N is the number of observations and p is the number of nuclides whose compositions are tracked.

Three methods were used to compare the test case to the training data:

1. Nearest Neighbor with L_1 norm
2. Nearest Neighbor with L_2 norm
3. Ridge Regression

The first two methods utilize the nearest neighbor approach, where a measure of dissimilarity/distance is calculated for each of the nuclide vectors in the training data. The minimum in the distance measure is found, and the responsible member of the training data is declared the best fit. The reactor type and burnup of this training observation is taken to be the predictions for the test case.

The distance measures for methods one and two are given as

$$D_i^{(1)} = \|x - \mu^{(i)}\|_1^2 = \sum_{j=1}^p |(x_j - \mu_j^{(i)})| \quad (7)$$

$$D_i^{(2)} = \|x - \mu^{(i)}\|_2^2 = \sum_{j=1}^p (x_j - \mu_j^{(i)})^2 \quad (8)$$

where x is the test case nuclide vector and $\mu^{(i)}$ is the i^{th} column of the training data, X .

To improve the fidelity of the burnup prediction using these two methods, after the best-fit member of the training data was found, a linear interpolation was performed between training points adjacent to the best-fit training sample.

Ridge Regression was also used to make burnup predictions. This is a standard linear regression with a penalty placed on the regression vector, $\beta \in \mathbb{R}^{(N \times (p+1))}$, to discourage overfitting³. Given the true burnup of each training case, y , minimizing the ridge regression objective gives the regression vector.

$$\min_{\beta} \left\{ \|y - [\mathbf{1} \ X]\beta\|_2^2 + \lambda \sum_{i=1}^p \beta_i^2 \right\} \quad (9)$$

where $\mathbf{1}$ is column vector of ones.

Ridge regression was chosen because it has a closed form solution and penalizing the regression vector makes it well suited for applications with correlated variables, which naturally arises in the analysis of radionuclides due to radioactive decay [9]. The ridge regression model was trained using the data without added error (see Section 3.2) using a validation set that was removed from the training data.

The average percent error in burnup prediction was recorded as a measure of the predictive power for each combination of nuclide subset and prediction technique.

Training and testing data was generated using ORIGEN-ARP 5.1.01 included in SCALE 6. The top 200 nuclides by mass at discharge were calculated for eleven PWR fuel types, nine BWR fuel types, and two PWHR fuel types using the cross sections included in ORIGEN-ARP. Decay calculations were performed for four different cooling times after discharge: one minute, seven days, thirty days, and one year.

For each combination of cooling time and fuel type, calculations were performed for a wide range of burnup values, corresponding to approximately one month to eighteen months of operation in one-month increments. Power densities of 32, 23, and 22 MW/MTU were used for the simulations of the PWRs, BWRs, and PHWRs, respectively. Burnup values used for PWR simulations were 600 to 17,700 MWd/MTU in steps of 950 MWd/MTU, and values of 600 to 12,330 in steps of 690 MWd/MTU were used for simulations of BWRs and PHWRs. This resulted in eighteen burnup values for the BWR and PHWR reactors and nineteen values for the PWR data. The basis, enrichment, and availability were kept constant between calculations, except in the case of the VVER and CANDU reactors, where enrichment is a key design difference. These values and average initial enrichment values were approximated from the literature [10-12]. Table 8 summarizes the training data simulations.

Table 8. Parameters used in ORIGEN-ARP to generate training data. Fuel types are referred to by their identifiers used in ORIGEN-ARP.

Fuel	Reactor	Enrichment [w/o]
CE14x14	PWR	2.8
CE16x16	PWR	2.8
W14x14	PWR	2.8
W15x15	PWR	2.8
W17x17	PWR	2.8
S14x14	PWR	2.8
VVER440(3.60)	PWR	3.60
VVER440(3.82)	PWR	3.82
VVER440(4.25)	PWR	4.25
VVER440(4.38)	PWR	4.38
VVER1000	PWR	2.8
GE7	BWR	2.9
GE8	BWR	2.9
GE9	BWR	2.9
GE10	BWR	2.9
Abb8	BWR	2.9
Atrium9	BWR	2.9
SVEA64	BWR	2.9
SVEA100	BWR	2.9
CANDU28	PHWR	0.711
CAND37	PHWR	0.711

Test cases were generated in the same way. Three reactors were used, and initial enrichments and cooling times that were and were not represented in the training data were simulated. Table 9 summarizes the test cases. In total, there were 1,628 samples in the training set and 62 in the testing set.

Table 9. Parameters for the generation of test case data in ORIGEN-ARP. Fuel types are referred to by their identifiers used in ORIGEN-ARP. Power densities are the same as the training data.

Fuel	Reactor	Enrichment [w/o]	Cooling Time	Burnup [MWd/MTU]
CANDU28	PHWR	0.711	{1m, 7d, 30d, 1a}	{1400, 5000, 11000}
CANDU28	PHWR	0.711	{3m, 9d, 2a}	{5000, 6120}
CE16x16	PWR	2.8	{1m, 7d, 30d, 1a}	{1700, 8700, 17000}
CE16x16	PWR	2.8	{3m, 9d, 2a}	{8700, 9150}
CE16x16	PWR	3.1	{7d, 9d}	{8700, 9150}
GE7	BWR	2.9	{1m, 7d, 30d, 1a}	{2000, 7200, 10800}
GE7	BWR	2.9	{3m, 9d, 2a}	{7200, 8800}
GE7	BWR	3.2	{7d, 9d}	{7200, 8800}

The top 200 nuclides by mass at discharge were recorded for each case. A master list of all the nuclides present in the nuclide vectors within the training data were pooled, and each of the nuclide vectors in the training and test set were sorted to follow this order. This yielded a total of 308 unique radionuclides. If a nuclide in the master list was not in a sample's top 200, a zero was used in that position of the formatted nuclide vector for that sample.

Nuclide Subsets. In order to ascertain subsets of nuclides that are most effective at making burnup predictions, Principle Components Analysis was performed to see which nuclides varied the most in the training data [9]. The nuclides that most contributed to the first two principle components along which burnup seemed to vary were selected and used to make predictions on the test cases. Additionally, predictions were made where actinides were ignored.

Effect of Error. The effect of measurement error was investigated by randomly perturbing the nuclide concentrations in the test case nuclide vectors and the effects on the accuracy of the burnup and reactor type predictions were noted. For each element of a test case nuclide vector, a random number in the interval $[1-E_{max}, 1+E_{max}]$ was chosen to form an error vector that was used to add error to test case nuclide vectors. The same error vector was used for each of the three methods. For each of the three nuclide lists (full, short, fission products), the set of test cases were analyzed with each of the three methods fifty times for each value of maximum error, i.e. fifty different random error vectors were generated, and the results averaged in order to gain statistical confidence in the results.

The results of PCA and the resulting shortened nuclide list used in the analyses are given in Table 10. Many of the identified fission products reside towards the edges of the bimodal fission yield curves. Additional identified nuclides are uranium, neptunium, and plutonium isotopes, which are directly affected by burnup and neutron flux [13].

Table 10. Nuclide list derived from PCA performed on the training data.

Nuclide	
^{138}Ba	^{103}Rh
^{140}Ce	^{101}Ru
^{142}Ce	^{102}Ru
^{144}Ce	^{104}Ru
^{133}Cs	^{150}Sm
^{135}Cs	^{88}Sr
^{137}Cs	^{90}Sr
^{139}La	^{99}Tc
^{95}Mo	^{130}Te
^{97}Mo	^{234}U
^{98}Mo	^{235}U
^{100}Mo	^{236}U
^{143}Nd	^{238}U
^{144}Nd	^{131}Xe
^{145}Nd	^{132}Xe
^{146}Nd	^{134}Xe
^{148}Nd	^{136}Xe
^{237}Np	^{89}Y
^{105}Pd	^{91}Zr
^{141}Pr	^{92}Zr
^{239}Pu	^{93}Zr
^{240}Pu	^{94}Zr
^{241}Pu	^{96}Zr
^{242}Pu	

Figure 3 shows the success rate of the reactor predictions using all three nuclide lists and the nearest neighbor methods. The results are averaged over all the test cases and fifty trials each. While the data is extremely noisy, a general downward trend towards minimum asymptotes at success rates of approximately 0.2903 and 0.3548 may be observed. When data without added error is used, the fission products nuclide list exhibits the poorest performance, but lines corresponding to these lists seems to approach the asymptote slower than the other nuclide-list/method combinations, which implies that measurements including actinides seems to perform the best but are most sensitive to measurement inaccuracies. Using the two lists including actinides, in order to achieve better than 50% success in reactor type predictions, the maximum error in nuclide measure must be less than 1%.

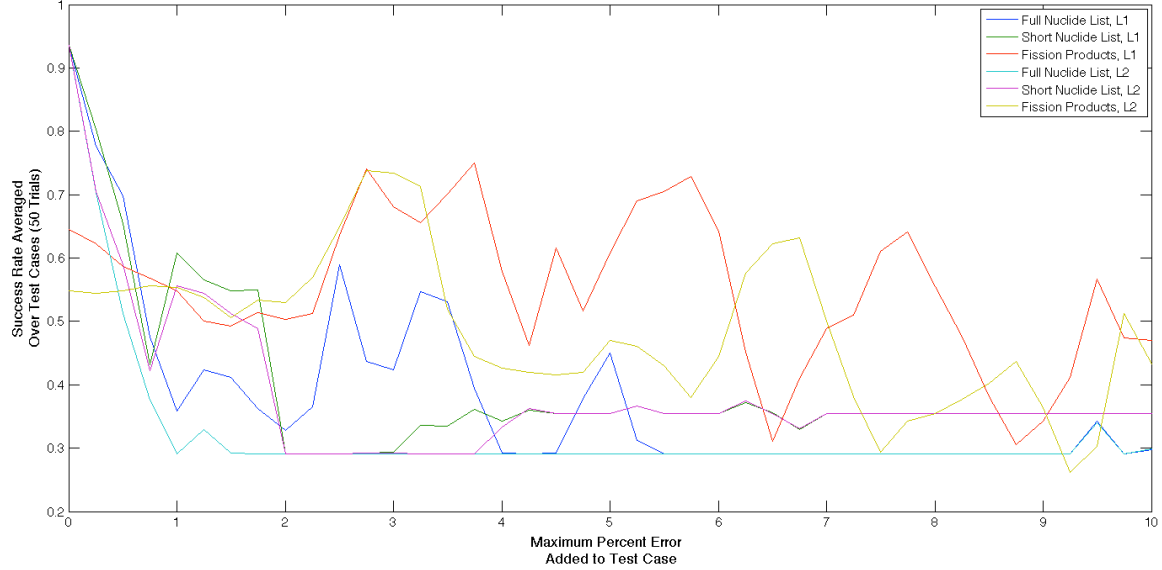


Figure 3. The success rate at predicting the reactor class (PWR, BWR, PHWR) on the test cases. Data shown is averaged over the 62 test cases and 50 trials/unique error vectors, which were used for both of the reactor type prediction methods as described in Section 3.2.

Figures 4 and 5 show the percent error in burnup predictions averaged over the test set and fifty trials. For small amounts of added error, ridge regression makes the most accurate predictions and does so until the maximum measurement error exceeds 1 or 2 percent. Not including actinides in the nuclide lists with the nearest neighbor approaches improves the algorithms' accuracy with clean data compared to the other nuclide lists. Additionally, the decline in performance with increasing measurement error is slowest using this “fission products” nuclide list. Furthermore, using the L_1 norm seems to yield better performance than the L_2 norm at all levels of test-case measurement error.

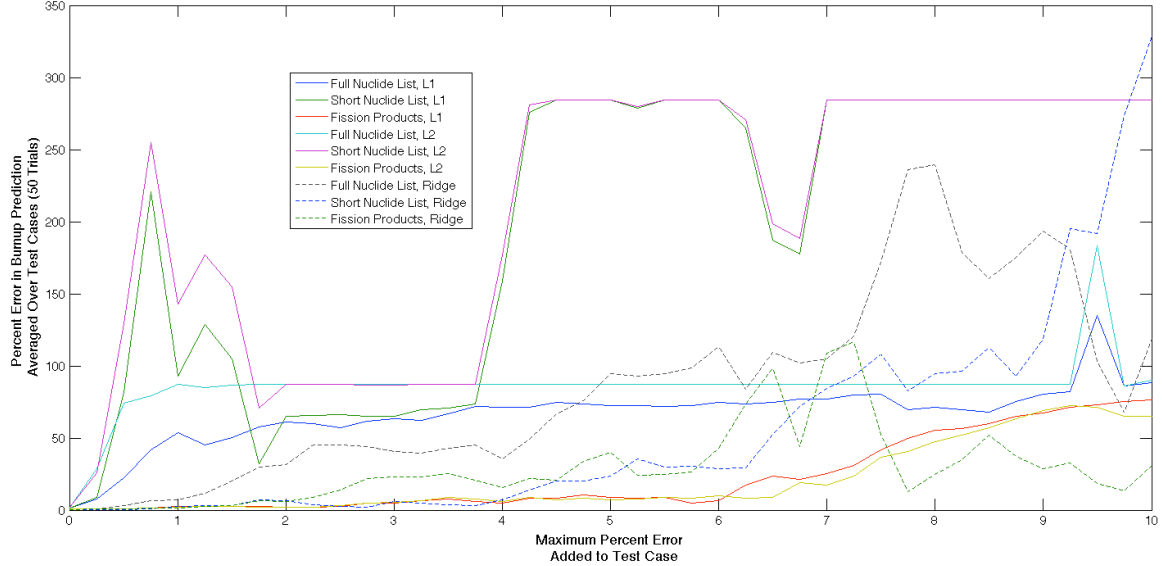


Figure 4. Average percent error in burnup predictions on the test cases. Data shown is averaged over the 62 test cases and 50 trials/unique error vectors, which were used for all of the predictions methods as described in Section 3.2.

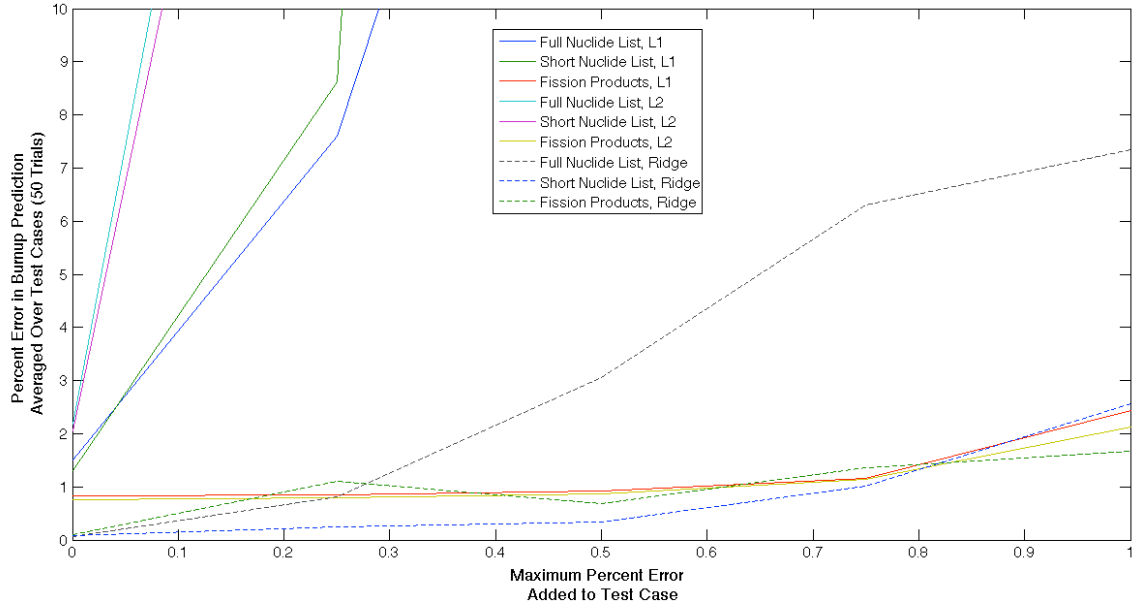


Figure 5. Detailed average percent error in burnup prediction on the test cases, zoomed into the region between 0 and 1 percent.

While this work is promising, it is by no means exhaustive. We outline several limitations of this study as disclaimers and suggestions for further work.

Analysis Methods. There is significant optimization that could be done with the methods employed, such as extending the first two analysis methods described in Section 2 to use more similar training data, i.e.,

k-nearest neighbors [9]. Additionally, there are other feature selection methods that could be employed to separate nuclides that are useful for predictions from those that are confusing, such as correlation analysis or sequential feature extraction methods, which could improve the predictive power of the methods employed in this study [9]. Moreover, there are numerous approaches to multivariate data analysis that offer many additional benefits to the simple approaches taken in this initial study, such as noise reduction and robustness to outliers and measurement error [9].

Data Preparation. There has been no examination in this work on the effect of using a smaller training set or measurement error in the training data, and how these issues could be mitigated, such as replicate measurements taken during the collection of training data. Also, the nuclide lists used in this study were formed without thought about detection methods and which radionuclides could be measured with reasonable accuracy and precision. Furthermore, the artificial error added to the test cases was done with a random distribution. A non-trivial improvement would be to add error sampled from a Poisson distribution while taking into account parent/daughter relationships.

Through this simple study of nearest neighbor and ridge regression algorithms to burnup and reactor class predictions using simulated nuclear composition vectors of simulated spent nuclear fuel, it has been demonstrated that good results can be obtained when the measurements are accurate to within 1%. These results suggest that investigation into refining these techniques by applying other analysis algorithms and more extensive testing multivariate data analysis's application to this and other forensics problems is warranted.

Task 4.9 Mass spectrometry measurement of ^{146}Sm and ^{151}Sm .

Radio-samarium samples were created for measurement in The University of Texas TRIGA reactor. ^{151}Sm is a nearly pure beta emitter apart from one low energy, low intensity gamma ray. It is difficult to detect this gamma peak in activated natural Sm which contains appreciable Compton interference and x-rays from the other activation products. Beta spectroscopy is also problematic as self-shielding effects and interferences from 6 beta rays of the ^{154}Sm activation product, ^{155}Eu , complicate the quantification of the underlying ^{151}Sm beta spectrum. The alternative approach to direct measurement compares measured values of a second activation product in the sample with solutions of the Bateman equations.

The ^{151}Sm content may be ascertained from gamma-ray spectra of ^{155}Eu which is produced from the activation of ^{154}Sm and subsequent decay of ^{155}Sm . The Bateman equations describing this set of reactions are

$$\frac{dN_{\text{Sm}151}}{dt} = F_{\gamma,\text{Sm}150}N_{\text{Sm}150} - (F_{a,\text{Sm}151} + \lambda_{\text{Sm}151})N_{\text{Sm}151} \quad (10)$$

$$\frac{dN_{\text{Sm}155}}{dt} = F_{\gamma,\text{Sm}154}N_{\text{Sm}154} - (F_{a,\text{Sm}155} + \lambda_{\text{Sm}155})N_{\text{Sm}155} \approx F_{\gamma,\text{Sm}154}N_{\text{Sm}154} - \lambda_{\text{Sm}155}N_{\text{Sm}155} \quad (11)$$

$$\frac{dN_{Eu155}}{dt} = \lambda_{Sm155} N_{Sm155} - \lambda_{Eu155} N_{Eu155} \quad (12)$$

The N terms are number densities, the F_γ terms are radiative capture rates, the F_a terms are absorption rates, and λ are decay constants. Note the approximation in equation 12. The 22.3 min half-life of ^{155}Sm results in a decay constant which is several orders of magnitude larger than the total absorption rate. Thus the contribution to losses due to absorption is negligible. It is assumed that for short to moderate irradiation times (days or less) the number densities of ^{150}Sm and ^{154}Sm remain very nearly constant. These equations may then be solved using Laplace transforms. The number density of ^{151}Sm is

$$N_{Sm151}(t) = \frac{F_{\gamma,Sm150} N_{Sm150}}{F_{a,Sm151} + \lambda_{Sm151}} [1 - e^{-(F_{a,Sm151} + \lambda_{Sm151})t}] \quad (13)$$

The ^{155}Eu number density is given by

$$N_{Eu155}(t) = \frac{F_{\gamma,Sm154} N_{Sm154}}{\lambda_{Eu155}} [1 + \frac{\lambda_{Eu155}}{\lambda_{Sm155} - \lambda_{Eu155}} e^{-\lambda_{Sm155}t} + \frac{\lambda_{Sm155}}{\lambda_{Eu155} - \lambda_{Sm155}} e^{-\lambda_{Eu155}t}] \quad (14)$$

Natural isotope number densities and decay constants were obtained from [14]. Capture and absorption rates were calculated from

$$F_i = \sum_{g=1}^G \phi_g \sigma_{i,g} \quad (15)$$

where i denotes the particular type of interaction (e.g. $\gamma, ^{151}\text{Sm}$), ϕ_g is the flux in the energy group g , $\sigma_{i,g}$ is the cross section for interaction of type i in energy group g , and G is the total number of energy groups. 63 group cross sections from the Cinder90 cross section library included in MCNPX 2.6 [15] were used as the $\sigma_{i,g}$. Group fluxes were calculated by means of MCNPX using a volumetric (F4) flux tally in a cell containing a cylinder of Sm(III) oxide. The size, position, and density of the cell were defined to replicate the material and geometric description of the sample irradiated in the TRIGA core. Using equation 7 is equivalent to using 1 group collapsed cross sections in the activation equations.

The irradiation consists of the irradiation of a 0.5 g of Sm(III) powder sample was irradiated in a rotary specimen rack facility (RSR) of the University of Texas (UT) at Austin's TRIGA Mark II reactor. The RSR is a rotating annular channel surrounding the fuel assembly. The powder was irradiated for 30 minutes at a reactor power of 950kW. This corresponds to a total neutron fluence of $5 \times 10^{15} \text{ cm}^{-2}$.

Quantification of the ^{155}Eu concentration was done by gamma ray spectroscopy. After decaying for several days, the irradiated Sm powder was counted on a high purity germanium detector (HPGe) for 24 hours in normal mode. Areas of the 86.5, 105.3 and 146.1 keV photopeaks were used to extrapolate the ^{155}Eu activity in the sample at the end of irradiation. In order to determine the decay rates of the 86.5 and 105.3 keV peaks, a low-energy efficiency curve was generated with calibrated ^{137}Cs and ^{57}Co sources.

The ^{151}Sm concentration was also estimated using burnup calculations within MCNPX 2.6. A model of UT Austin's TRIGA core was modified to include a BURN card. The BURN card couples burnup and activation calculations with a KCODE criticality calculation to iteratively adjust spectral changes in the flux and track the buildup of various nuclides. See [15] for more details. To reduce the computation time required to arrive at reasonable uncertainties, variance reduction was implemented by increasing the neutron importance of cells near the Sm cell. This includes a number of nested virtual cells which split each incoming neutron into two. Color maps of the neutron importance are shown, imposed over the core geometry, in figure 6. The virtual cells are the nested cylinders surrounding the Sm sample (the smallest blue cell). All other cells represent real geometric elements of the core.

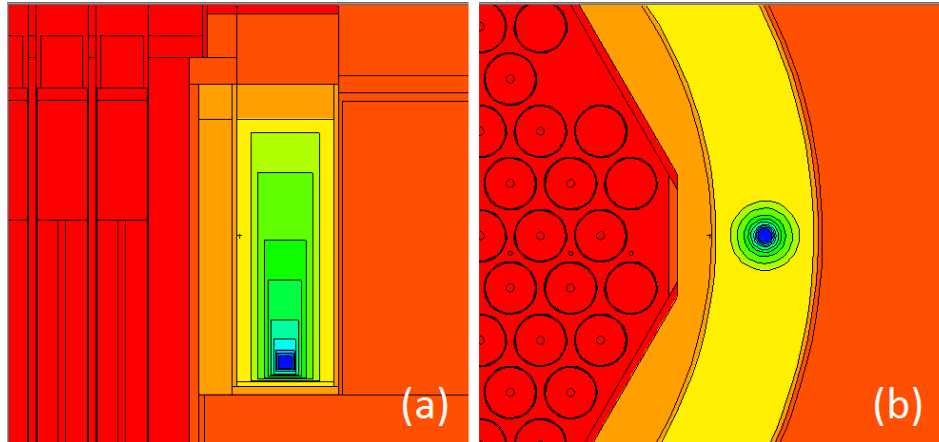


Figure 6: Neutron importance in the MCNPX model of the UT Austin's TRIGA core. (a) side view and (b) top view of sample in the rotary specimen rack (RSR) irradiation facility.

The Sm oxide powder was counted for 24 hours after a 29 day decay period. The activity concentration of ^{155}Eu extrapolated to the end of irradiation period was 17.7 ± 0.2 kBq/g. Equations 4 and 5 were used to estimate a $^{151}\text{Sm}/^{150}\text{Sm}$ ratio of $(1.35 \pm 0.15) \times 10^{-7}$ corresponding to the measured concentration of ^{155}Eu . The MCNPX burnup calculations estimated the ratio to be $(1.3 \pm 0.2) \times 10^{-7}$ and the ^{155}Eu concentration to be 20 ± 3 kBq/g. The calculated values for the ^{155}Eu concentration and the Sm ratio are shown as the solid black line in figure 7 and represent

solutions to the Bateman equations parameterized by the neutron fluence. The dotted black lines indicate the standard error propagated from the uncertainty of the flux. The yellow dot is located at the intersection of the measured ^{155}Eu concentration and the parametric curve. The corresponding value on the x-axis indicates the Sm ratio inferred from measurement. The red square indicates the values of the ^{155}Eu concentration and Sm ratio as determined from the output files of the MCNPX burnup calculations. Standard error bars on ^{155}Eu concentration and Sm ratio are displayed for each data point in figure 7. The error on the measured ^{155}Eu concentration, however, is too small to display. The combined average of both estimates is $(1.33 \pm 0.15) \times 10^{-7}$.

The MCNPX model ran 30 inactive KCODE cycles and 130 active cycles with 10000 sources particles per cycle. The run took 18 hours on a Pentium T4400 dual-core processor.

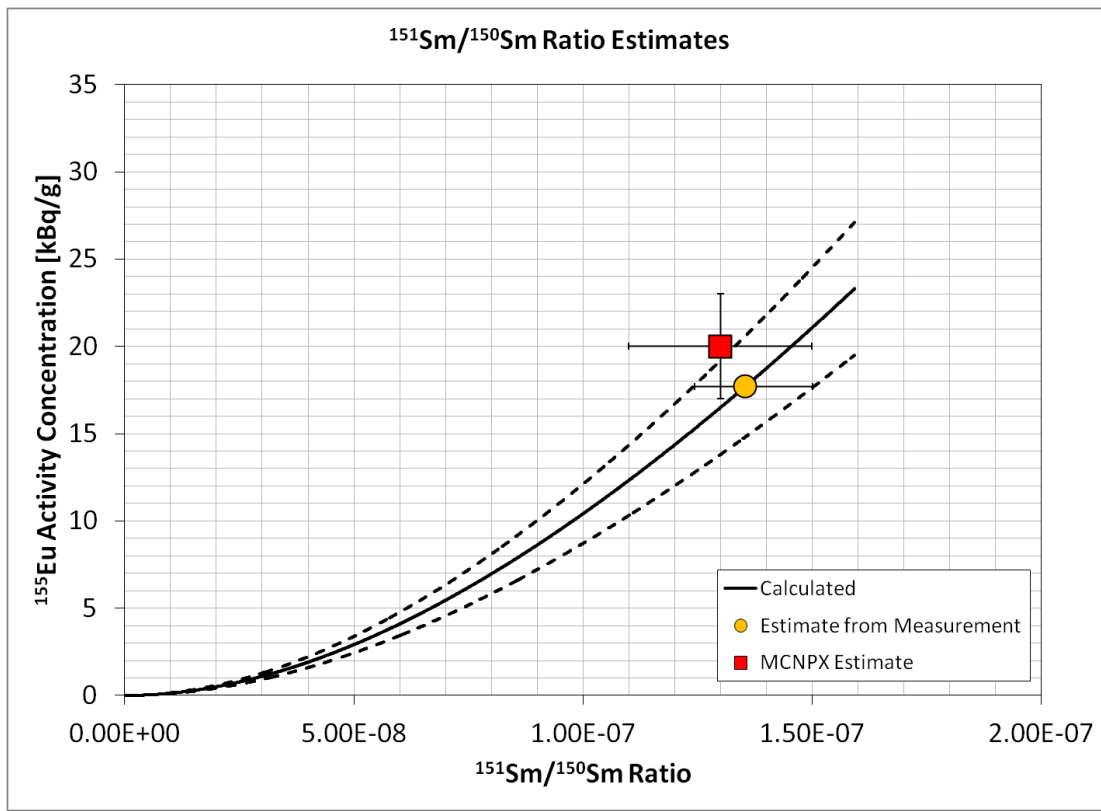


Figure 7: Sm ratio estimates made from measured values and MCNPX burnup calculations.

The Sm ratio estimated from the measured ^{155}Eu concentrations is in reasonable agreement with the value calculated with MCNPX. Large uncertainties are associated with the MCNPX results despite variance reduction efforts. This is attributed to the small size of the sample relative to the reactor geometry which results in a small probability of the Sm cell interacting with a source

neutron. Consequently the solution converges slowly relative to flux tallies in other cells but still orders of magnitude faster than with no variance reduction present.

Several naturally occurring Sm isotopes have unusually large absorption cross sections. ^{149}Sm for example has a 60232b Maxwell averaged cross section. Therefore, even a sample of Sm oxide powder as small as 1 gram can significantly perturb the neutron flux. The effects of neutron self-shielding greatly alter the spatially and energy dependent flux from its values in an infinitely dilute absorber. Using the ^{155}Eu concentration to estimate the Sm ratio is akin to using a flux monitor with the advantage that the homogeneously distributed ^{154}Sm accounts for any large spatial and spectral variations in the flux that contribute to the ^{150}Sm activation rate. Therefore, using ^{155}Eu to renormalize the flux only requires an accurate knowledge of the spectral shape in the neutron flux. This is usually within the capabilities of MCNPX.

^{151}Sm , prepared by neutron activation of Sm(III)oxide (Sm_2O_3) powder was quantified for future accelerator mass spectrometry measurements. Ratios of $^{151}\text{Sm}/^{150}\text{Sm}$ estimated by gamma spectrometry measurements of ^{155}Eu coupled with solutions of Bateman equations agreed with MCNPX burnup calculations. These two estimates yielded an average Sm ratio of $(1.33\pm0.15)\times10^{-7}$.

The irradiated Sm_2O_3 powder was shipped to LLNL for isotopic analyses. It was dissolved in Ultrex HCl ($<1\times10^{-12}$ Eu and Nd) to a concentration of 8 mg Sm/mL in 5% HCl. An aliquot of this stock solution was used to establish the detection limits by ICPMS described in Task 4.7. The stock solution was diluted with Sm ICP standard ($<1\times10^{-6}$ Eu) solution to produce solutions of different $^{151}\text{Sm}/^{150}\text{Sm}$ ratios. These diluted solutions, ICP standard solution, and non-irradiated Sm_2O_3 dissolved in HCl were prepared as SmF_3 samples as described in Task 4.4 with slight changes described below.

Table 11. Isotope ratios of $^{151}\text{Sm}/^{150}\text{Sm}$ in Sm solutions.

Sample Name	Sm concentration (mg/mL)	$^{151}\text{Sm}/^{150}\text{Sm}$
Working Stock	8.1	1.33×10^{-7}
Dilution 1	1.47	4.88×10^{-8}
Dilution 2	1.06	3.43×10^{-9}
Dilution 3	1.01	4.73×10^{-10}
Dilution 4	1.01	4.29×10^{-11}
Dilution 5	1.00	3.67×10^{-12}
Dilution 6	1.00	6.29×10^{-13}

Start with sufficient volume to have 3 mg Sm in solution. Add 3 mL 48% ultrex hydrofluoric acid ($<1\times10^{-12}$ Eu and Nd) and allow samarium fluoride to precipitate overnight. Centrifuge to form a pellet and remove the supernatant. Add 1 mL of dilute hydrofluoric acid, re-suspend the pellet and centrifuge again. Repeat rinse with dilute hydrofluoric acid and centrifuge 2 more

times. Dry precipitate overnight in a convection oven set at 85°C. Place dry SmF_3 in a watertight vial until ready to use. The day before measurement, mix each SmF_3 sample with Nb metal powder (Sm:Nb~3:1) and press into aluminum sample targets. The mass of SmF_3 was measured and indicated Sm recovery was 75-80%. Targets were also loaded with commercially available high purity SmF_3 powder ($<1 \times 10^{-6}$ Eu and Nd) mixed with Nb and used to tune the AMS system for the Sm beam. Place the targets in the ion source overnight to further dry the samples under vacuum. The ion source pressure is $<1 \times 10^{-6}$ Torr.

The AMS system was tuned using the $^{152}\text{SmF}_-$ produced by the ion source operating at a cathode voltage of 5.5 kV and extraction voltage of -40 kV. Approximately 80 μA of negative ions are produced by the source with 80 nA being $^{152}\text{SmF}_-$ after a low energy mass spectrometer. The ^{152}Sm isotope was selected because neither ^{151}Sm nor ^{153}Sm are found naturally. Thus, ^{152}Sm is well separated from tails of other stable Sm isotopes. The $^{152}\text{SmF}_-$ beam was accelerated through a potential of 7.5MV and sent through a thin foil to strip electrons to produce a distribution of positive charge states. At 7.5MV, the most populated charge states are 9+ and 10+, both at about 20%. We selected $^{152}\text{Sm}^{9+}$ because odd numbered charge states tend to have fewer interferences, so our high energy beam had an energy of 74.21 MeV. Substantial scattering occurs during passage through the stripping foil, so the focused beam intensity between the accelerator and high energy mass spectrometer is only about 150 nA despite each ion carrying a charge of 9+. After the high energy mass spectrometer, the $^{152}\text{Sm}^{9+}$ drops to only 1-2 nA, and is maintained through a electrostatic analyzer to the particle detector. The electrostatic analyzer is essentially an energy filter. These stable isotope currents were similar for AMS targets regardless of the starting source of Sm. The stable $^{152}\text{Sm}^{9+}$ was scaled to $^{151}\text{Sm}^{9+}$ and checked for current at Faraday cups throughout the AMS system. No current was measurable ($<1 \text{ pA}$) at mass 151 after the high energy spectrometer. The slits immediately after the low energy spectrometer were then completely wound in to stop the beam and all in beam Faraday cups were removed from the beam line. No counts were registered in the detector. The slit were then opened to 0.010 inches, 1/30th the aperture used for tuning. The detector registered a count rate of several hundred events per second, indicative of a stable isobar interference (^{151}Eu) or large tail of down scattered ^{150}Sm . There was no way to discern what caused the counts, and opening the slits any further would damage the detector.

The high count rate at mass 151 is very likely due to ^{151}Eu . The concentration of Eu in the various spec sheets was consistent with an Eu/Sm concentration around 1 ppm. This level is below or at detection limits of ICPMS but 100-1000x the levels tolerated by AMS. Measuring ^{151}Sm by AMS requires a significant improvement in the suppression of Eu, from the current 1×10^{-6} available to 1×10^{-9} to 1×10^{-12} . Achieving a reduction in stable Eu concentration of 4-6 orders of magnitude is a significant task, beyond the scope of this limited study. The lanthanides have similar chemistry and many stable isobars, real challenges to AMS. Serial ion chromatography separations is an approach, but it would be very labor intensive. The current

detector on the heavy element AMS beamline has limited dE/dx capabilities also, so an improved detector with greater resolution to resolve scattered tails would be helpful. An improved detector would provide better separation, but chemistry is the better target for improvement. Reducing interference isobar concentration to approximately the same order of magnitude as the target rare isotope is needed to make routine ^{151}Sm measurements.

Task 4.10 Conduct presentations/meetings at times and places specified in the contract schedule.

Two presentations were made at the Methods and Application in Radioanalytical Chemistry (MARC) in March 2012 and one presentation was made at the 2012 DTRA Basic Research Technical Review.

Task 4.11 Write Option Year 2 report.

A final report has been written and submitted by the September 1, 2012 deadline.

References

1. Joint Working Group of the American Physical Society and the American Association for the Advancement of Science, Nuclear Forensics: Role, State of the Art, and Program Needs (2007).
2. MOODY, K., HUTCHEON, I., GRANT, P. Nuclear Forensic Analysis. Taylor & Francis (2005).
3. WEAVER, C., BIEGALSKI, S., BUCHHOLZ, B., Assessment of non-traditional isotopic ratios by mass spectrometry for analysis of nuclear activities. *Journal of Radioanalytical and Nuclear Chemistry* (2009).
4. WHITNEY, S., BIEGALSKI, S., Analytical nuclear fuel cycles from isotopic ratios of waste products applicable to measurement by accelerator mass spectrometry. *Nuclear Science and Engineering* **157**, 200-209 (2007).
5. WILLMAN, C., HÅKANSSON, A., OSIFO, O., BÄCHLIN, A., SVÄRD, S., Nondestructive assay of spent nuclear fuel with gamma-ray spectroscopy. *Annals of Nuclear Energy* **33**, 427-438 (2006).
6. DIFOGLIO, R. Examination of some misconceptions about near-infrared analysis. *Applied Spectroscopy* **49**, 67-75 (1995).
7. OLIVIERI, A. Analytical advantages of multivariate data processing. *Analytical Chemistry* **80**, 5713-5720 (2008).
8. BEEBE, K., PELL, R., SEASHOLTZ. Chemometrics: A Practical Guide. John Wiley and Sons (1998).
9. HASTIE, T., TIBSHIRANI, R., FRIEDMAN, J. The Elements of Statistical Learning: Data Mining, Inference, and Predictions. Springer (2009).
10. ILAS, G., GAULD, I. Analysis of decay heat measurements for BWR fuel assemblies, Nuclear Fuels and Structural Materials for the Next Generation Nuclear Reactors, Reno, Nevada, June 4–8, 2006. *Trans. Am. Nucl. Soc.*, **94**, 385–387 (2006).
11. KNIEF, R. Nuclear Engineering: Theory and Technology of Commercial Nuclear Power. American Nuclear Society (2008).
12. MURPHY, B. ORIGEN-ARP Cross-Section Libraries for Magnox, Advanced Gas-Cooled, and VVER Reactor Designs, Oak Ridge National Laboratory (2004).
13. Chart of Nuclides (2012) National Nuclear Data Center, Brookhaven National Laboratory. <http://www.nndc.bnl.gov/chart/>. Accessed 12 February 2012
14. MCNPX 2.6.0 Manual (2012) MCNPX Homepage. mcnpx.lanl.gov/docs/MCNPX_2.6.0_Manual.pdf. Accessed 1 January 2012

Appendix

Table A1. Results of the analysis of the various test cases using FOM₁

Different Enrichment	Different Burnup	Different Cooling Time	Reactor Type Guess	Simulated Reactor	Success	Best-fit Burnup [MWd/MTU]	Error [%]	Interpolated Burnup [MWd/MTU]	Error [%]	Simulated Burnup [MWd/MTU]	Cooling Time Guess	Simulated Cooling Time	Success
	1		'candu28'	'CANDU28'	1	1290	7.86%	1552	10.86%	1400	'1years'	'1years'	1
	1		'candu37'	'CANDU28'		1290	7.86%	1522	8.71%	1400	'7days'	'1minutes'	
	1		'candu28'	'CANDU28'	1	1290	7.86%	1547	10.50%	1400	'30days'	'7days'	
	1		'candu28'	'CANDU28'	1	1290	7.86%	1552	10.86%	1400	'30days'	'30days'	1
	1		'candu37'	'CANDU28'		4740	5.20%	5318	6.36%	5000	'1years'	'1years'	1
	1		'candu37'	'CANDU28'		4740	5.20%	5301	6.02%	5000	'7days'	'1minutes'	
	1		'candu37'	'CANDU28'		4740	5.20%	5313	6.26%	5000	'30days'	'7days'	
	1		'candu37'	'CANDU28'		4740	5.20%	5318	6.36%	5000	'30days'	'30days'	1
	1		'candu28'	'CANDU28'	1	10950	0.45%	11046	0.42%	11000	'1years'	'1years'	1
	1		'candu28'	'CANDU28'	1	10950	0.45%	11047	0.43%	11000	'1minutes'	'1minutes'	1
	1		'candu28'	'CANDU28'	1	10950	0.45%	11047	0.43%	11000	'7days'	'7days'	1
	1		'candu28'	'CANDU28'	1	10950	0.45%	11047	0.43%	11000	'30days'	'30days'	1
	1	1	'candu37'	'CANDU28'		6120	0.00%	6129	0.15%	6120	'1years'	'2years'	1
	1	1	'candu37'	'CANDU28'		6120	0.00%	6129	0.15%	6120	'1minutes'	'3minutes'	1
	1	1	'candu37'	'CANDU28'		6120	0.00%	6130	0.16%	6120	'7days'	'9days'	1
	1	1	'candu37'	'CANDU28'		4740	5.20%	5318	6.36%	5000	'1years'	'2years'	1
	1	1	'candu37'	'CANDU28'		4740	5.20%	5302	6.04%	5000	'7days'	'3minutes'	
	1	1	'candu37'	'CANDU28'		4740	5.20%	5315	6.30%	5000	'30days'	'9days'	
	1		'ce16x16'	'CE16'	1	1550	8.82%	1909	12.29%	1700	'1years'	'1years'	1
	1		'ce16x16'	'CE16'	1	1550	8.82%	1889	11.12%	1700	'7days'	'1minutes'	
	1		'ce16x16'	'CE16'	1	1550	8.82%	1905	12.06%	1700	'30days'	'7days'	
	1		'ce16x16'	'CE16'	1	1550	8.82%	1909	12.29%	1700	'30days'	'30days'	1
	1		'vver1000'	'CE16'		9150	5.17%	8307	4.52%	8700	'1years'	'1years'	1
	1		'vver1000'	'CE16'		9150	5.17%	8317	4.40%	8700	'1minutes'	'1minutes'	1
	1		'vver1000'	'CE16'		9150	5.17%	8334	4.21%	8700	'1minutes'	'7days'	
	1		'vver1000'	'CE16'		9150	5.17%	8309	4.49%	8700	'30days'	'30days'	1
	1		'w14x14'	'CE16'		16750	1.47%	17198	1.16%	17000	'1years'	'1years'	1
	1		'w14x14'	'CE16'		16750	1.47%	17206	1.21%	17000	'1minutes'	'1minutes'	1
	1		'w14x14'	'CE16'		16750	1.47%	17196	1.15%	17000	'30days'	'7days'	
	1		'w14x14'	'CE16'		16750	1.47%	17201	1.18%	17000	'30days'	'30days'	1
	1	1	'vver1000'	'CE16'		9150	5.17%	8308	4.51%	8700	'1years'	'2years'	1
	1	1	'vver1000'	'CE16'		9150	5.17%	8317	4.40%	8700	'1minutes'	'3minutes'	1
	1	1	'vver1000'	'CE16'		9150	5.17%	8313	4.45%	8700	'7days'	'9days'	1
	1	1	'ce16x16'	'CE16'	1	9150	0.00%	9154	0.04%	9150	'1years'	'2years'	1
	1	1	'ce16x16'	'CE16'	1	9150	0.00%	9164	0.15%	9150	'1minutes'	'3minutes'	1
	1	1	'ce16x16'	'CE16'	1	9150	0.00%	9152	0.02%	9150	'30days'	'9days'	
1	1		'ge10'	'CE16'		8880	2.07%	8467	2.68%	8700	'7days'	'7days'	1
1	1	1	'ge10'	'CE16'		8880	2.07%	8464	2.71%	8700	'30days'	'9days'	
1			'ge10'	'CE16'		8880	2.95%	9125	0.27%	9150	'30days'	'7days'	
1		1	'ge10'	'CE16'		8880	2.95%	9126	0.26%	9150	'30days'	'9days'	
	1		'ge7'	'GE7'	1	1980	1.00%	2062	3.10%	2000	'1years'	'1years'	1
	1		'ge7'	'GE7'	1	1980	1.00%	2054	2.70%	2000	'1minutes'	'1minutes'	1
	1		'ge7'	'GE7'	1	1980	1.00%	2060	3.00%	2000	'7days'	'7days'	1
	1		'ge7'	'GE7'	1	1980	1.00%	2061	3.05%	2000	'30days'	'30days'	1
	1		'ge8'	'GE7'		7500	4.17%	6922	3.86%	7200	'1years'	'1years'	1
	1		'ge8'	'GE7'		7500	4.17%	6913	3.99%	7200	'1minutes'	'1minutes'	1
	1		'ge8'	'GE7'		7500	4.17%	6932	3.72%	7200	'1minutes'	'7days'	
	1		'ge8'	'GE7'		7500	4.17%	6938	3.64%	7200	'1minutes'	'30days'	
	1		'ge7'	'GE7'	1	10950	1.39%	10666	1.24%	10800	'1years'	'1years'	1
	1		'ge7'	'GE7'	1	10950	1.39%	10658	1.31%	10800	'1minutes'	'1minutes'	1
	1		'ge7'	'GE7'	1	10950	1.39%	10662	1.28%	10800	'7days'	'7days'	1
	1		'ge7'	'GE7'	1	10950	1.39%	10669	1.21%	10800	'7days'	'30days'	
	1	1	'ge7'	'GE7'	1	8880	0.00%	8910	0.34%	8880	'1years'	'2years'	1
	1	1	'ge7'	'GE7'	1	8880	0.00%	8900	0.23%	8880	'1minutes'	'3minutes'	1
	1	1	'ge7'	'GE7'	1	8880	0.00%	8906	0.29%	8880	'7days'	'9days'	1
	1	1	'ge8'	'GE7'		7500	4.17%	6923	3.85%	7200	'1years'	'2years'	1
	1	1	'ge8'	'GE7'		7500	4.17%	6913	3.99%	7200	'1minutes'	'3minutes'	1
	1	1	'ge8'	'GE7'		7500	4.17%	6933	3.71%	7200	'1minutes'	'9days'	
1			'ge10'	'GE7'		8190	7.77%	8252	7.07%	8880	'1minutes'	'7days'	
1		1	'ge10'	'GE7'		8190	7.77%	8255	7.04%	8880	'1minutes'	'9days'	
1	1		'ge10'	'GE7'		6120	15.00%	6637	7.82%	7200	'7days'	'7days'	1
1	1	1	'ge10'	'GE7'		6120	15.00%	6638	7.81%	7200	'7days'	'9days'	1

Table A2. Results of the analysis of the various test cases using FOM₂

Different Enrichment	Different Burnup	Different Cooling Time	Reactor Type Guess	Simulated Reactor	Success	Best-fit Burnup [MWd/MTU]	Error [%]	Interpolated Burnup [MWd/MTU]	Error [%]	Simulated Burnup [MWd/MTU]	Cooling Time Guess	Simulated Cooling Time	Success
	1		'candu28'	'CANDU28'	1	1290	7.86%	1441	2.93%	1400	'1years'	'1years'	1
	1		'candu28'	'CANDU28'	1	1290	7.86%	1411	0.79%	1400	'7days'	'1minutes'	
1			'candu28'	'CANDU28'	1	1290	7.86%	1442	3.00%	1400	'7days'	'7days'	1
1			'candu28'	'CANDU28'	1	1290	7.86%	1441	2.93%	1400	'30days'	'30days'	1
1			'candu28'	'CANDU28'	1	4740	5.20%	5188	3.76%	5000	'1years'	'1years'	1
1			'candu37'	'CANDU28'		4740	5.20%	5127	2.54%	5000	'7days'	'1minutes'	
1			'candu28'	'CANDU28'	1	4740	5.20%	5194	3.88%	5000	'7days'	'7days'	1
1			'candu28'	'CANDU28'	1	4740	5.20%	5192	3.84%	5000	'30days'	'30days'	1
1			'candu28'	'CANDU28'	1	10950	0.45%	11006	0.05%	11000	'1years'	'1years'	1
1			'candu28'	'CANDU28'	1	10950	0.45%	11014	0.13%	11000	'1minutes'	'1minutes'	1
1			'candu28'	'CANDU28'	1	10950	0.45%	11012	0.11%	11000	'7days'	'7days'	1
1			'candu28'	'CANDU28'	1	10950	0.45%	11010	0.09%	11000	'30days'	'30days'	1
1			'candu37'	'CANDU28'		6120	0.00%	6142	0.36%	6120	'1years'	'2years'	1
1			'candu37'	'CANDU28'		6120	0.00%	6140	0.33%	6120	'1minutes'	'3minutes'	1
1			'candu37'	'CANDU28'		6120	0.00%	6144	0.39%	6120	'7days'	'9days'	1
1	1		'candu28'	'CANDU28'	1	4740	5.20%	5192	3.84%	5000	'1years'	'2years'	1
1	1		'candu37'	'CANDU28'		4740	5.20%	5127	2.54%	5000	'7days'	'3minutes'	
1	1		'candu28'	'CANDU28'	1	4740	5.20%	5142	2.84%	5000	'30days'	'9days'	
1	1		'ce16x16'	'CE16'	1	1550	8.82%	1755	3.24%	1700	'1years'	'1years'	1
1	1		'ce16x16'	'CE16'	1	1550	8.82%	1733	1.94%	1700	'7days'	'1minutes'	
1	1		'ce16x16'	'CE16'	1	1550	8.82%	1743	2.53%	1700	'30days'	'7days'	
1	1		'ce16x16'	'CE16'	1	1550	8.82%	1756	3.29%	1700	'30days'	'30days'	1
1	1		'ce14x14'	'CE16'		9150	5.17%	8634	0.76%	8700	'1years'	'1years'	1
1	1		'ce14x14'	'CE16'		9150	5.17%	8647	0.61%	8700	'7days'	'1minutes'	
1	1		'ce14x14'	'CE16'		9150	5.17%	8613	1.00%	8700	'30days'	'7days'	
1	1		'ce14x14'	'CE16'		9150	5.17%	8674	0.30%	8700	'30days'	'30days'	1
1	1		'ce16x16'	'CE16'	1	16750	1.47%	17098	0.58%	17000	'1years'	'1years'	1
1	1		'ce16x16'	'CE16'	1	16750	1.47%	17042	0.25%	17000	'30days'	'1minutes'	
1	1		'ce16x16'	'CE16'	1	16750	1.47%	17084	0.49%	17000	'30days'	'7days'	
1	1		'ce16x16'	'CE16'	1	16750	1.47%	17129	0.76%	17000	'30days'	'30days'	1
1	1		'ce14x14'	'CE16'		9150	5.17%	8635	0.75%	8700	'1years'	'2years'	1
1	1		'ce14x14'	'CE16'		9150	5.17%	8647	0.61%	8700	'7days'	'3minutes'	
1	1		'ce14x14'	'CE16'		9150	5.17%	8622	0.90%	8700	'30days'	'9days'	
1	1		'ce16x16'	'CE16'	1	9150	0.00%	9147	0.03%	9150	'1years'	'2years'	1
1	1		'ce16x16'	'CE16'	1	9150	0.00%	9143	0.08%	9150	'7days'	'3minutes'	
1	1		'ce16x16'	'CE16'	1	9150	0.00%	9139	0.12%	9150	'30days'	'9days'	
1	1		'ge10'	'CE16'		8880	2.07%	8719	0.22%	8700	'7days'	'7days'	1
1	1	1	'ge10'	'CE16'		8880	2.07%	8730	0.34%	8700	'7days'	'9days'	1
1	1		'ge10'	'CE16'		8880	2.95%	9460	3.39%	9150	'7days'	'7days'	1
1	1		'ge10'	'CE16'		8880	2.95%	9484	3.65%	9150	'7days'	'9days'	1
1			'ge7'	'GE7'	1	1980	1.00%	2018	0.90%	2000	'1years'	'1years'	1
1			'ge7'	'GE7'	1	1980	1.00%	2005	0.25%	2000	'1minutes'	'1minutes'	1
1			'ge7'	'GE7'	1	1980	1.00%	2012	0.60%	2000	'7days'	'7days'	1
1			'ge7'	'GE7'	1	1980	1.00%	2016	0.80%	2000	'30days'	'30days'	1
1			'atrium10'	'GE7'		7500	4.17%	7004	2.72%	7200	'1years'	'1years'	1
1			'ge9'	'GE7'		6810	5.42%	7306	1.47%	7200	'1minutes'	'1minutes'	1
1			'atrium10'	'GE7'		7500	4.17%	7023	2.46%	7200	'1minutes'	'7days'	
1			'atrium10'	'GE7'		7500	4.17%	7036	2.28%	7200	'7days'	'30days'	
1			'ge7'	'GE7'	1	10950	1.39%	10772	0.26%	10800	'1years'	'1years'	1
1			'ge7'	'GE7'	1	10950	1.39%	10714	0.80%	10800	'1minutes'	'1minutes'	1
1			'ge7'	'GE7'	1	10950	1.39%	10770	0.28%	10800	'1minutes'	'7days'	
1			'ge7'	'GE7'	1	10950	1.39%	10783	0.16%	10800	'7days'	'30days'	
1			'ge7'	'GE7'	1	8880	0.00%	8901	0.24%	8880	'1years'	'2years'	1
1			'ge7'	'GE7'	1	8880	0.00%	8856	0.27%	8880	'1minutes'	'3minutes'	1
1			'ge7'	'GE7'	1	8880	0.00%	8873	0.08%	8880	'7days'	'9days'	1
1	1		'atrium10'	'GE7'		7500	4.17%	7011	2.63%	7200	'1years'	'2years'	1
1	1		'ge9'	'GE7'		6810	5.42%	7306	1.47%	7200	'1minutes'	'3minutes'	1
1	1		'atrium10'	'GE7'		7500	4.17%	7035	2.29%	7200	'1minutes'	'9days'	
1			'ge10'	'GE7'		8880	0.00%	8524	4.01%	8880	'1minutes'	'7days'	
1		1	'ge10'	'GE7'		8880	0.00%	8537	3.86%	8880	'1minutes'	'9days'	
1	1		'ge9'	'GE7'		6810	5.42%	7067	1.85%	7200	'1minutes'	'7days'	
1	1	1	'ge9'	'GE7'		6810	5.42%	6965	3.26%	7200	'7days'	'9days'	1

Following is some of the code in the form of m-files used to perform Task 4.3:

```
function makeOrigenInp(File_Name, Fuel_Type, Enrichment, Burnup, ...
    S_Power, Num_cycles, Mod_Den, Basis, T_c, T_c_units, Out_units, ...
    NRank, Location)

%Kenneth Dayman--University of Texas at Austin, PNNL--May 2011
%This function takes input parameters and writes a *.inp file for input
%into OrigenArp (via Scale6) for batch runs

%%%%%%%%%%%%%%%
%%%%%%%%%%%%%%%
%Input parameters:
%File_Name: Name of input file and the subsequent saved output after
%    running Origen
%Fuel_Type: The type of fuel assembly in OrigenArp shorthand,
%    e.g., ce14x14
%Enrichment: U-235 enrichment of the fuel in percent, e.g., 5
%Burnup: Desired final burnup of the fuel after N cycles
%S_Power: Power produced per unit fuel (MW/MTU) ~ power level of
%    reactor
%Num_Cycles: Number of cycles to use (1 or 3 typically)
%Mod_Den: Density of the moderator (Non-variable for many reactors),
%    g/cc
%Basis: Amount of uranium basis in grams
%T_c: Cooling time
%T_c_units: Units of the cooling time parameter (seconds, minutes,
%    months, years)
%Out_units: Units of the plot/out, e.g., grams, Curies, etc.
%NRank: Number of nuclides to be output, max 200
%Location: Directory where the .inp will be located and where the
%    Origen output will be saved

%%%%%%%%%%%%%%%
%%%%%%%%%%%%%%%
%Defines derived variables and arrays needed in the .inp file from the
%input parameters

%Hard-Wired Variables for Certain Reactors
```

```

if strcmpi(Fuel_Type,'ce14x14')
    Mod_Den = 0.7332;
elseif strcmpi(Fuel_Type,'ce16x16')
    Mod_Den = 0.71;
elseif strcmpi(Fuel_Type,'w14x14')
    Mod_Den = 0.7264;
elseif strcmpi(Fuel_Type,'s14x14')
    Mod_Den = 0.7283;
elseif strcmpi(Fuel_Type,'w15x15')
    Mod_Den = 0.7135;
elseif strcmpi(Fuel_Type,'w17x17')
    Mod_Den = 0.723;
elseif strcmpi(Fuel_Type,'w17x17_ofa')
    Mod_Den = 0.71;
elseif strcmpi(Fuel_Type,'vver440(3.6)')
    Enrichment = 3.6;
    Mod_Den = 0.75;
elseif strcmpi(Fuel_Type,'vver440(3.82)')
    Mod_Den = 0.75;
    Enrichment = 3.82;
elseif strcmpi(Fuel_Type,'vver440(4.25)')
    Mod_Den = 0.75;
    Enrichment = 4.25;
elseif strcmpi(Fuel_Type,'vver440(4.38)')
    Mod_Den = 0.75;
    Enrichment = 4.38;
elseif strcmpi(Fuel_Type,'vver1000')
    Mod_Den = 0.7145;
elseif strcmpi(Fuel_Type, 'agr')
    Mod_Den = 1;
elseif strcmpi(Fuel_Type, 'magnox')
    Mod_Den = 1;
elseif strcmpi(Fuel_Type, 'candu37')
    Mod_Den = 0.8121;
    Enrichment = 0.711;
elseif strcmpi(Fuel_Type, 'candu28')
    Mod_Den = 0.8121;
    Enrichment = 0.711;
end

```

```

time_of_cycle = (Burnup/Num_cycles)/S_Power;
power = S_Power*(Basis/1e6);
time_of_cycle_inc = time_of_cycle/10;
tempBasis = 1e6;
factor = Basis/tempBasis;

%computes the number of atoms of each U isotope, rounding to achieve a
%total of 1e6 atoms
u234 = round(((9e-05)*Enrichment+9e-9)*tempBasis);
u235 = round(Enrichment*tempBasis/100);
u236 = round(0.516854*u234);
%changed to tempBasis to avoid getting a negative amount of u238
u238 = tempBasis - u236 - u235 - u234;

%rescales the number of each U isotope to get the recover the desired
%basis
u234 = u234*factor;
u235 = u235*factor;
u236 = u236*factor;
u238 = u238*factor;

%Write the *.inp file
%prints the arp block
fid = fopen(strcat(File_Name,'.inp'),'w');
fprintf(fid, '=arp\r\n');
fprintf(fid, '%s',Fuel_Type);
fprintf(fid, '\r\n');
fprintf(fid, '%g',Enrichment);
fprintf(fid, '\r\n');
fprintf(fid, '%d',Num_cycles);
fprintf(fid, '\r\n');

for i = 1:Num_cycles
if time_of_cycle < 10
    fprintf(fid, '%0.6f',time_of_cycle);
    fprintf(fid,'r\n');
elseif time_of_cycle < 100
    fprintf(fid, '%0.5f',time_of_cycle);
    fprintf(fid,'r\n');
elseif time_of_cycle < 1000

```

```

fprintf(fid, '%0.4f,time_of_cycle);
fprintf(fid,'r\n');
elseif time_of_cycle < 10000
    fprintf(fid, '%0.3f,time_of_cycle);
    fprintf(fid,'r\n');
end
end

for i = 1:Num_cycles
    fprintf(fid,'%g',S_Power);
    fprintf(fid,'r\n');
end

for i = 1:Num_cycles
    fprintf(fid, '1\r\n');
end

fprintf(fid,'%g',Mod_Den);
fprintf(fid,'r\n');
fprintf(fid,'ft33f001\r\n');
fprintf(fid,'end\r\n');

%prints the origens block
fprintf(fid,'#origens\r\n');
fprintf(fid,'0$$ a4 33 a11 71 e t\r\n');
fprintf(fid, '%s',Fuel_Type);
fprintf(fid,'r\n');
fprintf(fid,'3$$ 33 a3 1 27 a16 2 a33 18 e t\r\n');
fprintf(fid,'35$$ 0 t\r\n');
fprintf(fid,'56$$ 10 10 a10 0 a13 4 a15 3 a18 1 e\r\n');
fprintf(fid,'57** 0 a3 1e-05 1 e\r\n');
fprintf(fid,'95$$ 0 t\r\n');
fprintf(fid,'Cycle 1 -');
fprintf(fid,'%s',File_Name);
fprintf(fid,'r\n');
fprintf(fid, '%g',Basis/1e6);
fprintf(fid,' MTU\r\n');
fprintf(fid,'58** ');

for i = 1:5
    fprintf(fid,'%g',power);

```

```

fprintf(fid,' ');
end
fprintf(fid, '\r\n ');
for i = 1:5
    fprintf(fid,'%g',power);
    fprintf(fid,' ');
end
fprintf(fid,'r\n');
fprintf(fid,'60** ');
j = 0;
for i = 1:10
    if i == 6
        fprintf(fid,'\r\n ');
    end
    j = j + time_of_cycle_inc;
    if j < 10
        fprintf(fid, '%0.6f',j);
        fprintf(fid,' ');
    elseif j < 100
        fprintf(fid, '%0.5f',j);
        fprintf(fid,' ');
    elseif j < 1000
        fprintf(fid, '%0.4f',j);
        fprintf(fid,' ');
    elseif j < 10000
        fprintf(fid, '%0.3f',j);
        fprintf(fid,' ');
    end
end

if T_c == .1
    num_time_points = 7;
elseif T_c > .1 && T_c <= .3
    num_time_points = 6;
elseif T_c > .3 && T_c <= 1
    num_time_points = 7;
elseif T_c > 1 && T_c <= 3
    num_time_points = 8;
elseif T_c > 3 && T_c <= 10
    num_time_points = 9;

```

```

elseif T_c > 10
    num_time_points = 8;
end

fprintf(fid,'r\n');
fprintf(fid,'66$$ a1 2 a5 2 a9 2 e\r\n73$$ 922340 922350 922360 922380\r\n');
fprintf(fid, '74** ');
fprintf(fid, '%g',u234);
fprintf(fid, ' ');
fprintf(fid, '%g',u235);
fprintf(fid, ' ');
fprintf(fid, '%g',u236);
fprintf(fid, ' ');
fprintf(fid, '%g',u238);
fprintf(fid, 'r\n');
fprintf(fid,'75$$ 2 2 2\r\n');
fprintf(fid,'t\r\n');
fprintf(fid,'54$$ a8 1 a11 0 e\r\n');
fprintf(fid,'56$$ a2 ');
fprintf(fid,'%d',num_time_points);
fprintf(fid,' a6 1 a10 10 ');
if strcmpi(T_c_units,'seconds')
    fprintf(fid, 'a14 1 ');
elseif strcmpi(T_c_units, 'minutes')
    fprintf(fid, 'a14 2 ');
elseif strcmpi(T_c_units, 'hours')
    fprintf(fid, 'a14 3 ');
elseif strcmpi(T_c_units, 'years')
    fprintf(fid, 'a14 5 ');
end
fprintf(fid, 'a15 3 a17 2 e\r\n');
fprintf(fid,'57** 0 a3 1e-05 e\r\n');
fprintf(fid,'95$$ 0 t\r\n');
fprintf(fid,'Cycle 1 Down - ');
fprintf(fid,"%s",File_Name);
fprintf(fid,'r\n');
fprintf(fid, '%g',Basis/1e6);
fprintf(fid,' MTU\r\n');
fprintf(fid,'60** ');

```

```

%CHECK THIS BLOCK
if T_c == .1
    num_time_points = 7;
    fprintf(fid, '0.0001 0.0003 0.001 0.003 0.01 0.03 ');
    fprintf(fid,"%g",T_c);
elseif T_c > .1 && T_c <= .3
    num_time_points = 6;
    fprintf(fid, '0.001 0.003 0.01 0.03 0.1 ');
    fprintf(fid,"%g",T_c);
elseif T_c > .3 && T_c <= 1
    num_time_points = 7;
    fprintf(fid,'0.001 0.003 0.01 0.03 0.1 0.3 ');
    fprintf(fid,"%g",T_c);
elseif T_c > 1 && T_c <= 3
    num_time_points = 8;
    fprintf(fid, '0.001 0.003 0.01 0.03 0.1 0.3 1 ');
    fprintf(fid,"%g",T_c);
elseif T_c > 3 && T_c <= 10
    num_time_points = 9;
    fprintf(fid, '0.001 0.003 0.01 0.03 0.1 0.3 1 3 ');
    fprintf(fid,"%g",T_c);
elseif T_c > 10
    num_time_points = 8;
    fprintf(fid, '0.01 0.03 0.1 0.3 1 3 10 ');
    fprintf(fid,"%g",T_c);
end
%END BLOCK

fprintf(fid,'r\n');
fprintf(fid,'61** f0.05r\n');
fprintf(fid,'65$$r\n');
fprintf(fid,'"Gram-Atoms Grams Curies Watts-All Watts-Gamma\r\n');
fprintf(fid,' 3z 1 0 0 3z 3z 3z 6z\r\n');
fprintf(fid,' 3z 1 0 0 3z 3z 3z 6z\r\n');
fprintf(fid,' 3z 1 0 0 3z 3z 3z 6z\r\n');
fprintf(fid,'81$$ 2 0 26 1 a7 200 e\r\n');
fprintf(fid, '82$$ ');

for i = 1:num_time_points
    fprintf(fid, '2 ');

```

```

end

fprintf(fid, 'e\r\n');
fprintf(fid,'83**\r\n');
fprintf(fid,' 1.000000e+07     8.000000e+06     6.500000e+06     5.000000e+06
4.000000e+06\r\n');
fprintf(fid,' 3.000000e+06     2.500000e+06     2.000000e+06     1.660000e+06
1.330000e+06\r\n');
fprintf(fid,' 1.000000e+06     8.000000e+05     6.000000e+05     4.000000e+05
3.000000e+05\r\n');
fprintf(fid,' 2.000000e+05 1.000000e+05 5.000000e+04 1.000000e+04 e\r\n');
fprintf(fid,'84**\r\n');
fprintf(fid,' 2.000000e+07 6.434000e+06 3.000000e+06 1.850000e+06\r\n');
fprintf(fid,' 1.400000e+06     9.000000e+05     4.000000e+05     1.000000e+05
1.700000e+04\r\n');
fprintf(fid,' 3.000000e+03     5.500000e+02     1.000000e+02     3.000000e+01
1.000000e+01\r\n');
fprintf(fid,' 3.0499900e+00     1.7700000e+00     1.2999900e+00     1.1299900e+00
1.000000e+00\r\n');
fprintf(fid,' 8.000000e-01 4.000000e-01 3.250000e-01 2.250000e-01 9.9999850e-02\r\n');
fprintf(fid,' 5.000000e-02 3.000000e-02 9.9999980e-03 1.000000e-05 e\r\n');
fprintf(fid,'t\r\n');

for i = 1:num_time_points
    fprintf(fid,'56$$ 0 0 a10 ');
    fprintf(fid,'%g',i);
    fprintf(fid,' e t\r\n');
end
fprintf(fid,'56$$ f0 t\r\n');
fprintf(fid,'end\r\n');
fprintf(fid,'=opus\r\n');
fprintf(fid,'LIBUNIT=33\r\n');
fprintf(fid,'TYPARAMS=NUCLIDES\r\n');
Out_units = upper(Out_units);
fprintf(fid,'UNITS=');
fprintf(fid,'%s',Out_units);
fprintf(fid,' \r\n');
fprintf(fid,'LIBTYPE=ALL\r\n');
fprintf(fid,'TIME=');
T_c_units = upper(T_c_units);

```

```

fprintf(fid,'%s',T_c_units);
fprintf(fid,'r\n');
fprintf(fid,'NPOSITION=');
for i = 1:num_time_points
    fprintf(fid,'%g',i);
    fprintf(fid,' ');
end
fprintf(fid,'end\r\n');
fprintf(fid,'NRANK=(');
fprintf(fid,'%d',NRank);
fprintf(fid,')\r\n');
fprintf(fid,'end\r\n');
fprintf(fid,'#shell\r\n');
fprintf(fid,'copy ft71f001 "");
fprintf(fid,'%s',Location);
fprintf(fid,'\\');
fprintf(fid,'%s',File_Name);
fprintf(fid,'.f71"\r\n');
fprintf(fid,'del ft71f001\r\n');
fprintf(fid,'end');

fclose(fid);
end

```

```

function [Database,MasterNuclide,newNames] = makeDTRAdatabase()
    %Kenneth Dayman -- University of Texas at Austin -- June 2011
    %
    %This function opens each ORIGEN run listed in the batch file, and compiles
    %the nuclide and mass information into a usable database for use in inverse
    %calculations for identifying fuel cycles (defined here as ordered triples:
    %(reactor_type, cooling time, burnup))
    %
    %A MasterNuclideList is compiled from all the nuclides observed in the
    %output of the ORIGEN runs. The data from each run is then compiled into
    %an (N x 1628) matrix, where N is the number of nuclides in the
    %MasterNuclideList and 1628 is the number of runs. If a particular run
    %does not exhibit a nuclide in the MasterNuclideList, a zero will be
    %inserted. The ordering of each run (column) is preserved to ensure that
    %each row only contains data relating to a single nuclide.

```



```

%MasterNuclides = Listing of all the nuclides accounted for in the
%      Database
%names = all the fuel cycles accounted for in the Database
%FoM type = {'square' => least squares Figure of Merit
%      'abs' => absolute value Figure of Merit
%      'relative' => relative absolute value Figure of Merit
%      (possibly ill-defined due to divide by 0's}

%Reads in the Names and masses of the unknown ORIGEN output
longname = strcat(unknownFileName,'_plot000.plt');
fid = fopen(char(longname));
if numTimePoints == 6
    temp = textscan(fid, '%s %*f %*f %*f %*f %*f %*f','HeaderLines',6);
elseif numTimePoints == 7
    temp = textscan(fid, '%s %*f %*f %*f %*f %*f %*f %*f','HeaderLines',6);
elseif numTimePoints == 8
    temp = textscan(fid, '%s %*f %*f %*f %*f %*f %*f %*f %*f','HeaderLines',6);
elseif numTimePoints == 9
    temp = textscan(fid, '%s %*f %*f %*f %*f %*f %*f %*f %*f %*f','HeaderLines',6);
end

RunNuclides = temp{1};
RunMass = temp{2};
fclose(fid);
NumMasterNuclides = length(MasterNuclide);
NumNuclides = 200;
%Conforms the mass numbers to MasterNuclides order and full listing.
%If a nuclide in MasterNuclides is not in the unkown, then a 0 is
%listed. If a nuclide is the unknown is not in the MasterNuclides
%(very unlikely), that nuclide will be compared against a 0 external of
%the database in the calculating of the figures of merit
unknownFull = zeros(length(MasterNuclide),1);
NumNotPresent = 0;
NotPresentMasses = zeros(1,1);

for j = 1:NumMasterNuclides
    for k = 1:NumNuclides
        if strcmpi(RunNuclides(k),MasterNuclide(j))
            unknownFull(j) = RunMass(k);
        end
    end
end

```

```

    end
end

%checks for stuff in RunNuclides not in MasterNuclide and saves any
%nonPresentNuclides in NotPresentMasses for use later in calc. FoM's
for k = 1:NumNuclides
    notThere = 1;
    for j = 1:NumMasterNuclides
        if strcmpi(RunNuclides(k),MasterNuclide(j))
            notThere = 0;
            break;
        end
    end
    if notThere == 1;
        NotPresentMasses(NumNotPresent + 1) = RunMass(k);
        NumNotPresent = NumNotPresent + 1;
    end
end

%finds FoM for each known fuel cycle in the Database
FoM = zeros(1,length(names));
for i = 1:length(names)
    if strcmpi(FoMtype,'square')
        FoM(i) = sum((unknownFull-Database(:,i)).*(unknownFull-Database(:,i))); %FoM
    elseif strcmpi(FoMtype,'abs')
        FoM(i) = sum(abs(unknownFull-Database(:,i)));
    elseif strcmpi(FoMtype,'relative')
        FoM(i) = sum(abs(unknownFull-Database(:,i))./Database(:,i));
    else
        fprintf('Invalid Figure of Merit type');
    end

    if NumNotPresent ~= 0
        for j = 1:NumNotPresent
            if strcmpi(FoMtype,'square')
                FoM(i) = FoM(i) + (NotPresentMasses(j)^2); %FoM
            elseif strcmpi(FoMtype,'abs')
                FoM(i) = FoM(i) + abs(NotPresentMasses(j));
            elseif strcmpi(FoMtype,'relative')
                fprintf('nuclides not found in Database ignored. FoM undefined');
            else

```

```

        fprintf('Invalid Figure of Merit type');
    end
end
end
end

%Finds Minimum FoM and Declares that the best-fit fuel cycle (number i)
smallFoM = FoM(1);
winner = 1;
for i=2:length(FoM)
    if FoM(i)<smallFoM
        smallFoM = FoM(i);
        winner = i;
    end
end

%Parses name(i) to give reactor type and cooling time
tempparts = regexp(names(winner),'_','split');
parts = tempparts{1};
reactor_type = parts(1);
cooling_time = parts(3);
guessBurnup = str2double(parts(2));

%Interpolates burnup estimate from the i+1 and i-1 fuel cycles' burnups
if (guessBurnup ~= 600 && guessBurnup ~= 17700) || (guessBurnup ~= 600 && guessBurnup
~= 12330)
    temptemp1 = regexp(names(winner-1),'_','split');
    temp1=temptemp1{1};
    temptemp2 = regexp(names(winner+1),'_','split');
    temp2=temptemp2{1};
    burn1 = str2double(temp1(2));
    burn2 = str2double(temp2(2));
    d1 = abs(FoM(winner)-FoM(winner-1));
    d2 = abs(FoM(winner)-FoM(winner+1));
    interpBurnup = (d1/(d1+d2))*(burn2-burn1) + burn1;
else
    interpBurnup = 0;
end
end

```

DISTRIBUTION LIST
DTRA-TR-15-31

DEPARTMENT OF DEFENSE

DEFENSE THREAT REDUCTION
AGENCY
8725 JOHN J. KINGMAN ROAD
STOP 6201
FORT BELVOIR, VA 22060
ATTN: D. PETERSEN

DEFENSE TECHNICAL
INFORMATION CENTER
8725 JOHN J. KINGMAN ROAD,
SUITE 0944
FT. BELVOIR, VA 22060-6201
ATTN: DTIC/OCA

**DEPARTMENT OF DEFENSE
CONTRACTORS**

QUANTERION SOLUTIONS, INC.
1680 TEXAS STREET, SE
KIRTLAND AFB, NM 87117-5669
ATTN: DTRIAC